AN ELECTROCHEMICAL STUDY OF PYRRHOTITE

BY

KYOSUKE JIBIKI

B.Eng. Hokkaido University, 1966.

M. Eng. Hokkaido University, 1968.

A THESIS SUBMITTED IN PARTIAL FULFILMENT OF

THE REQUIREMENTS FOR THE DEGREE OF

MASTER OF APPLIED SCIENCE

in the Department

of

METALLURGY

We accept this thesis as conforming to the

required standard

THE UNIVERSITY OF BRITISH COLUMBIA

February, 1971

In presenting this thesis in partial fulfilment of the requirements for an advanced degree at the University of British Columbia, I agree that the Library shall make it freely available for reference and study. I further agree that permission for extensive copying of this thesis for scholarly purposes may be granted by the Head of my Department or by his representatives. It is understood that copying or publication of this thesis for financial gain shall not be allowed without my written permission.

Department of   **Metallurgy**

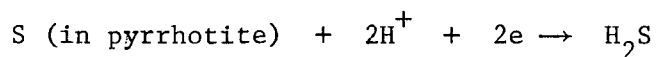The University of British Columbia
Vancouver 8, Canada

Date   **April 28, 1971**

ABSTRACT

The rest potential of sulphide electrodes was examined from both thermodynamic and kinetic aspects. The kinetic aspect has been found to be necessary for the interpretation of the establishment of the mixed potential in polyelectrode system, to which most sulphide systems belong.

The pyrrhotite electrode system was studied by measuring the rest potential while changing the concentrations of ferrous ion, hydrogen ion and hydrogen sulphide in the electrolyte, and the composition of pyrrhotite.

A mixed potential of pyrrhotite consisting of the reaction

$$S \text{ (in pyrrhotite)} + 2H^+ + 2e \longrightarrow H_2S$$

as a cathodic process and the reaction

$$Fe \text{ (in pyrrhotite)} \longrightarrow Fe^{++} + 2e$$
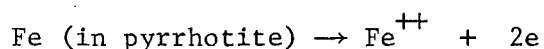
as an anodic process accounts for the dependence of the rest potential on those ionic species in the electrolyte and the composition of pyrrhotite electrodes.

ACKNOWLEDGEMENT

TABLE OF CONTENTS

LIST OF TABLES

LIST OF FIGURES

I. INTRODUCTION

The electrochemical properties of sulphide minerals in aqueous solution, which were first examined in the last century, have been studied mainly by geologists who determined electrode potentials of many sulphide minerals. From a practical point of view these works succeeded in arranging sulphides in a series of potentials analogous to the electrochemical series of metals. However, the potentials of sulphides measured were poorly reproducible and inconsistent with the values calculated from thermochemical data, and in fact, the meaning of electrode potentials of sulphides is not precisely understood today.

Meanwhile, these electrochemical properties of sulphides have been utilized in the study of various hydrometallurgical processes, e.g. electrolysis, leaching and flotation. Anodic electrolysis of sulphides yields metal ions and elementary sulphur or sulphate ions as products. The electrolysis of nickel matte is already commercialized, and known as the Hybinette process. Galvanic action may occur between particles of different sulphides in a slurry, analogous to galvanic corrosion between different metals; this was first noticed during geologic studies of mineral deposits.

Some attempts were made to interpret leaching reactions of sulphides as electrochemical processes, similar to the corrosion process

of metals which is now reasonably well understood. The application of pH-potential diagrams to the sulphide systems by various workers yields much information of a thermodynamic kind. However, all of the works undertaken to date failed to show the experimental validity of the pH-potential diagram. One of the possibilities for this is that kinetic considerations were largely ignored.

A full understanding of the electrochemical kinetic behaviour of sulphides is necessary before the properties of systems studied over a short time interval (shorter than geological time) can be completely understood for extractive metallurgy purposes. Thus some processes that come to equilibrium over a period of years, may be safely ignored in determining a useful diagram for extraction purposes, but then the diagram is one which may contain metastable phases, thermodynamically speaking, which do not react appreciably in allowed periods of time.

II. SIGNIFICANCE OF THE PRESENT WORK

The present work was undertaken to obtain the systematic measurement of the rest potentials of sulphides which were interpreted in terms of electrochemical kinetics rather than final thermodynamic equilibria.

In addition to these measurements, an attempt was made to obtain thermodynamic data of sulphides which were necessary for the more quantitative interpretation of electrochemical data.

Pyrrhotite, $Fe_{1-\alpha}S$ ($\alpha \ll 1$), was chosen as the sulphide in which the present work was undertaken. Although pyrrhotite is not as important as pyrite for metallurgical purposes because of its rarer occurrence in natural ores, it is often accompanied by nickel sulphide ores and the electrochemical behaviour seems to be closely related to that of pyrite. Only a few works have been reported on electrochemical studies of pyrrhotite. Pyrrhotite appears in a non-stoichiometric compound with a wide range of Fe:S ratio forming an iron deficient lattice, this non-stoichiometry of pyrrhotite may be expected to have an effect on the electrochemical behaviour of the minerals.

III. A REVIEW OF THE LITERATURE

(1) Description of Pyrrhotite

1) The Fe-S phase diagram

Although the Fe-S binary system has been studied in fair detail
from liquidus temperatures down to about 300°C, the low temperature
phase relationships are less well understood because of difficulty
with sluggish reaction rates. Nevertheless, in Fig. 1 the phase
relationships of the system at low temperatures are shown based on
phases observed in nature and on a limited number of laboratory
studies.[1]

According to Fig. 1 it can be seen that at low temperature the
phase relationships are more complicated than those at high temperature.

On cooling to 320 ± 5°C, the high temperature hexagonal pyrrhotite
passes through an inversion to low temperature hexagonal pyrrhotite.
The temperature of this inversion does not seem to be influenced by the
composition of the pyrrhotite.

Further cooling near the FeS composition leads to a second
inversion at 139°C and the troilite phase becomes stable. It is noted
in Fig. 1 that the troilite stability is very restricted both in regard
to composition, which cannot deviate from the stoichiometric FeS
and in regard to temperature. In fact, a recent work done by R. Yund
and H. Hall[2] showed that troilite appears to be restricted to the
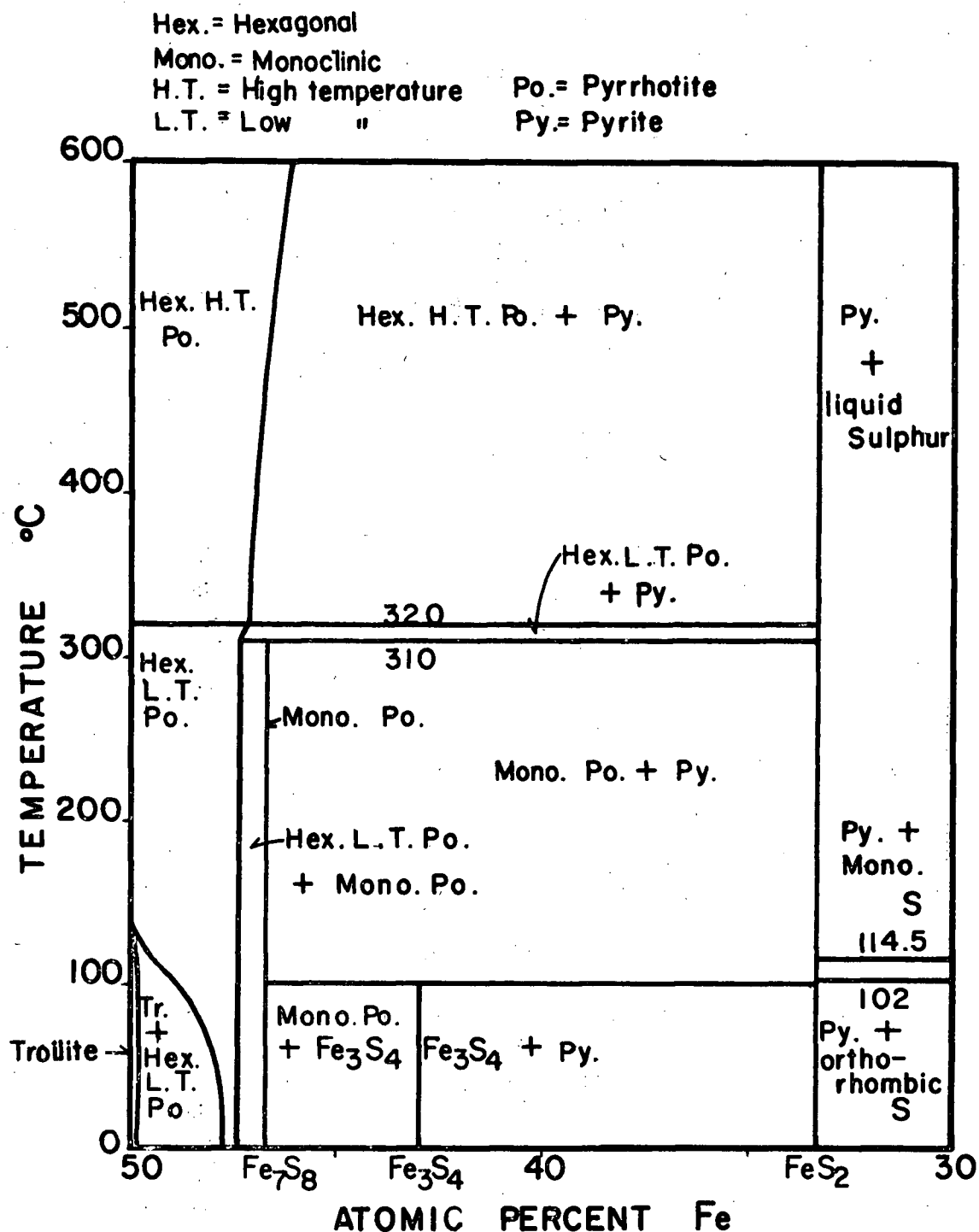
Figure 1. Tentative diagram of Fe-S system at low temperatures.
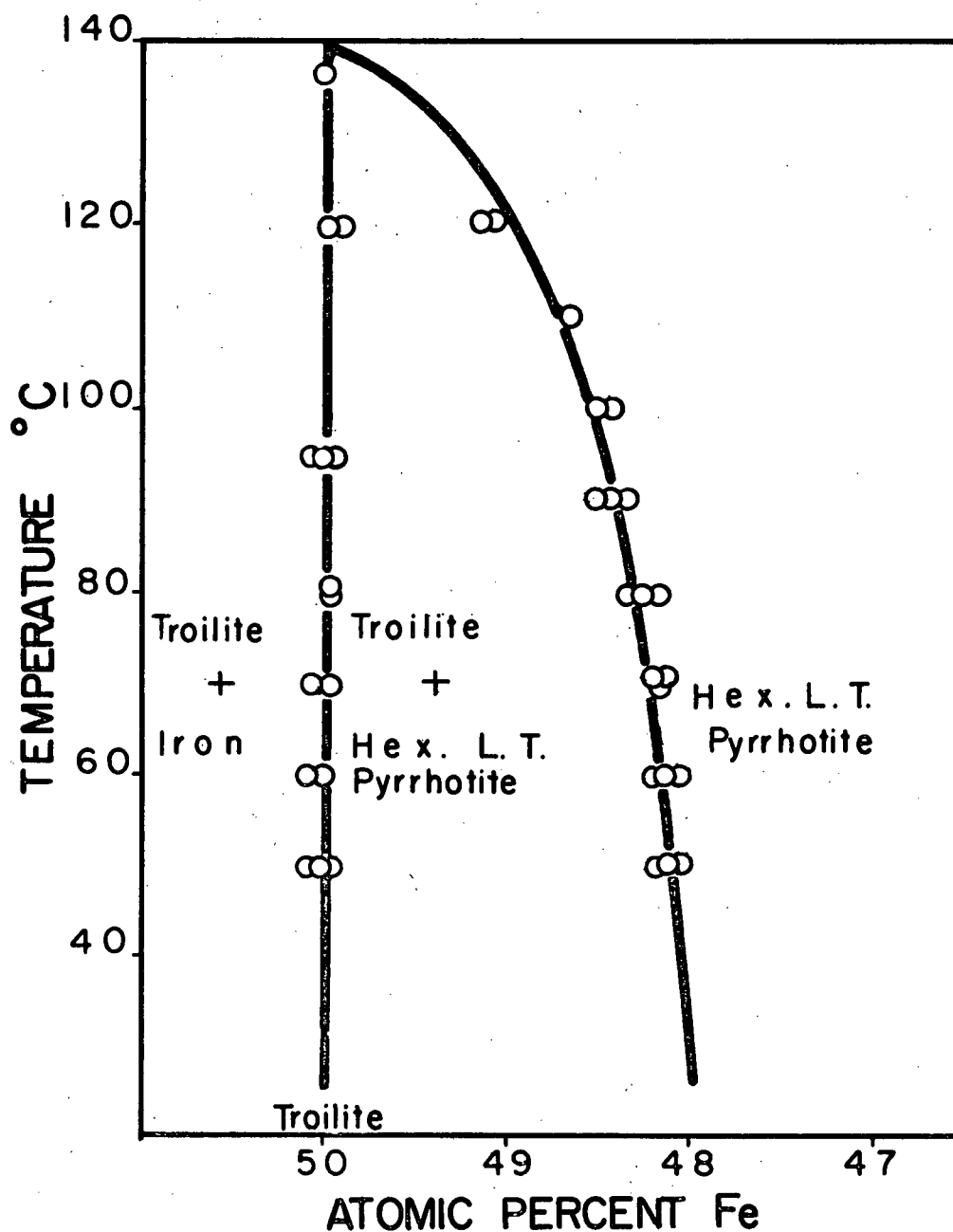
Figure 2. Details of the Fe-S diagram in the vicinity of troilite
and pyrrhotite.

stoichiometric FeS, shown in Fig. 2.

The univariant field existing below 139°C between troilite and the low temperature hexagonal pyrrhotite increases significantly in width with decreasing temperature. These two phases commonly co-exist in many ores.

A monoclinic pyrrhotite was first found in a number of Swedish ores. It has gradually become apparent that this mineral is quite common in ore deposits. Monoclinic pyrrhotite has been synthesized in the pure Fe-S system, being stable below 310°C in the presence of sulphur vapour. In Fig. 1 it is tentatively shown as a stable phase below 310°C. The compositions of numerous monoclinic pyrrhotites have been found to vary only slightly; the range is 46.45 to 46.70 atomic percent Fe. Monoclinic pyrrhotite and low-temperature hexagonal pyrrhotite form a common assemblage in natural ores as evidenced by X-ray powder diffraction studies. Monoclinic pyrrhotite-marcasite assemblages are found to be quite common in ores. A phase with Fe_3S_4 composition and rhombohedral structure was first reported and named smythite in 1957. However, its stability region is not confirmed yet, so in Fig. 1 a breakdown of the Fe_3S_4 compound is indicated tentatively at about 100°C.

In natural ores pyrite as well as marcasite is very common as the iron disulphide phase. However, the pyrite-marcasite relation has been a puzzle for many years. In composition there is a difference between the two minerals, indicated by numerous experiments, i.e. the orthorhombic marcasite contains less sulphur than the cubic pyrite which is essentially stoichiometric FeS_2. This account for the fact

that, when marcasite is heated with elemental sulphur under confining

pressure it converts to pyrite in a matter of days, at temperatures

even as low as 150°C, forming a pyrite rim around individual marcasite

grains. Several other studies on these minerals indicate that hydrogen

apparently plays an important role in the formation of marcasite

because both marcasite and pyrite form in Fe-S-O-H experiments but

pyrite only forms in Fe-S-O experiments. Although more extensive studies

need to be done, it now appears that the H-S bond may stabilize the

marcasite structure. For these reasons marcasite is not shown as a

phase in the pure Fe-S system.

2) Thermodynamic diagrams

Thermodynamic considerations yield information on the stable

phases in the Fe-S system to appear in selected environments. Because

sulphur as one of components of the Fe-S system is a very active element,

its activity in the environment determines the phase to be stabilized.

To date, although many studies have been made on the thermodyanmic

properties of the Fe-S system at high temperatures, studies at low

temperatures are not available. However, the data at high temperature

can be extrapolated to approximate the thermodynamic properties of

sulphides at low temperature.

The sulphur activities can be calculated as a function of composition

across the composition ranges, shown in the phase diagram of Fig. 1, by

using the existing thermodynamic data.[*] In Fig. 3 the sulphur activities

---

[*] In this work, unless otherwise state, all thermodynamic data were
obtained from "Oxidation Potentials" by Latimer.
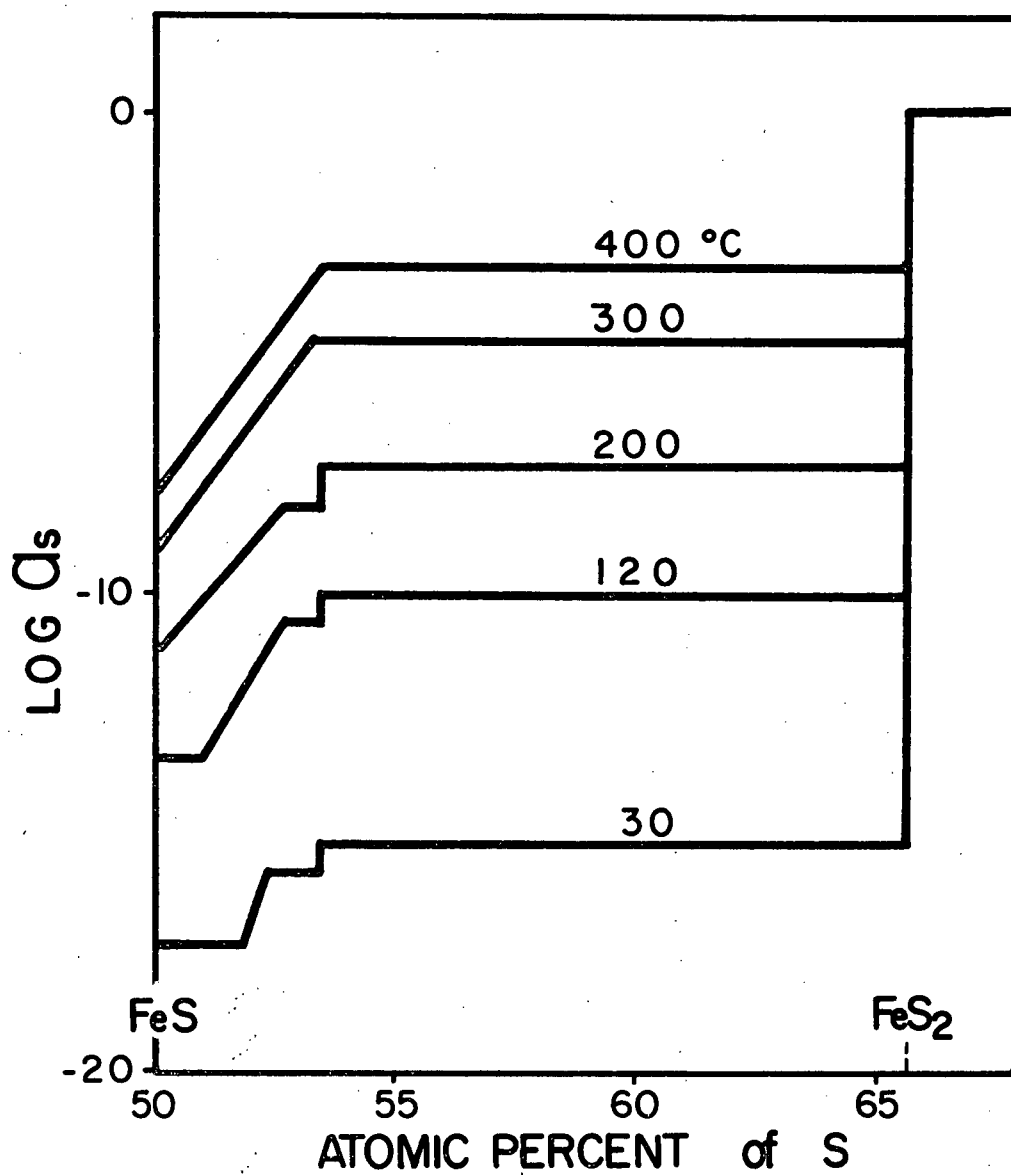
Figure 3. Schematic diagram of activity of sulphur in the Fe-S system.

were calculated at 400°C, and are shown schematically for lower

temperature regions corresponding to different phase relationships.

3) pH-Potential diagrams for iron sulphide

The pH-potential diagram shows a stable region of each phase in

the Fe-S system in aqueous environments from a thermodynamic point of

view.

3-1) Equilibrium pH-potential diagram

Fig. 4 shows the pH-potential diagram in acid regions made by

H. Majima.[4] The ferrous ion concentration is 1 M and 10^{-3} M to make

the diagram more applicable to practical considerations, concentrations

of other solutes are 1 M. In this figure, the pyrrhotite domain is a

small region, compared with pyrite.

3-2) Meta-stable pH-potential diagram

In practice the pyrrhotite phase persists at potentials and pH's

where pyrite is stable because of the extremely slow formation of pyrite

from pyrrhotite. Sulphur that is left on pyrrhotite during oxidation

does not react in laboratory times with unreacted pyrrhotite to form

pyrite. In Fig. 5 with this consideration the meta-stable pH-potential

diagram for pyrrhotite in acid regions is shown by H. Majima.[4] This

diagram is applicable only to iron-saturated pyrrhotite, which is

stoichiometric pyrrhotite, because the free enthalpy value used is of

pyrrhotite saturated with iron. For non-stoichiometric pyrrhotite, if

thermodynamic data are available, the same metal-stable diagrams

can be drawn. The domain for pyrrhotite of composition $Fe_{0.87}S$ is

drawn to indicate the change in stability due to compositional changes
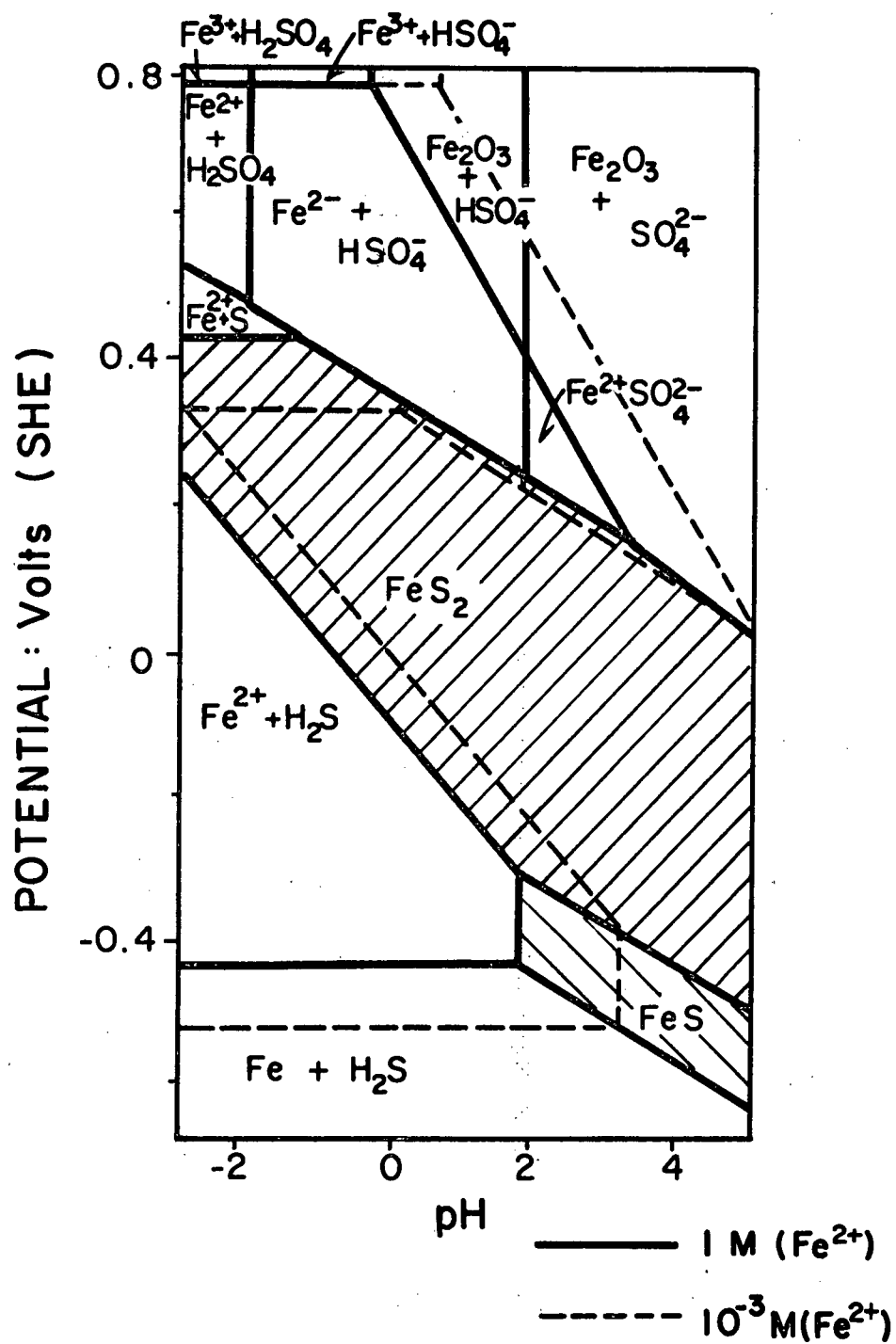
Figure 4. Potential-pH diagram for stable Fe-S systems at 25°C.
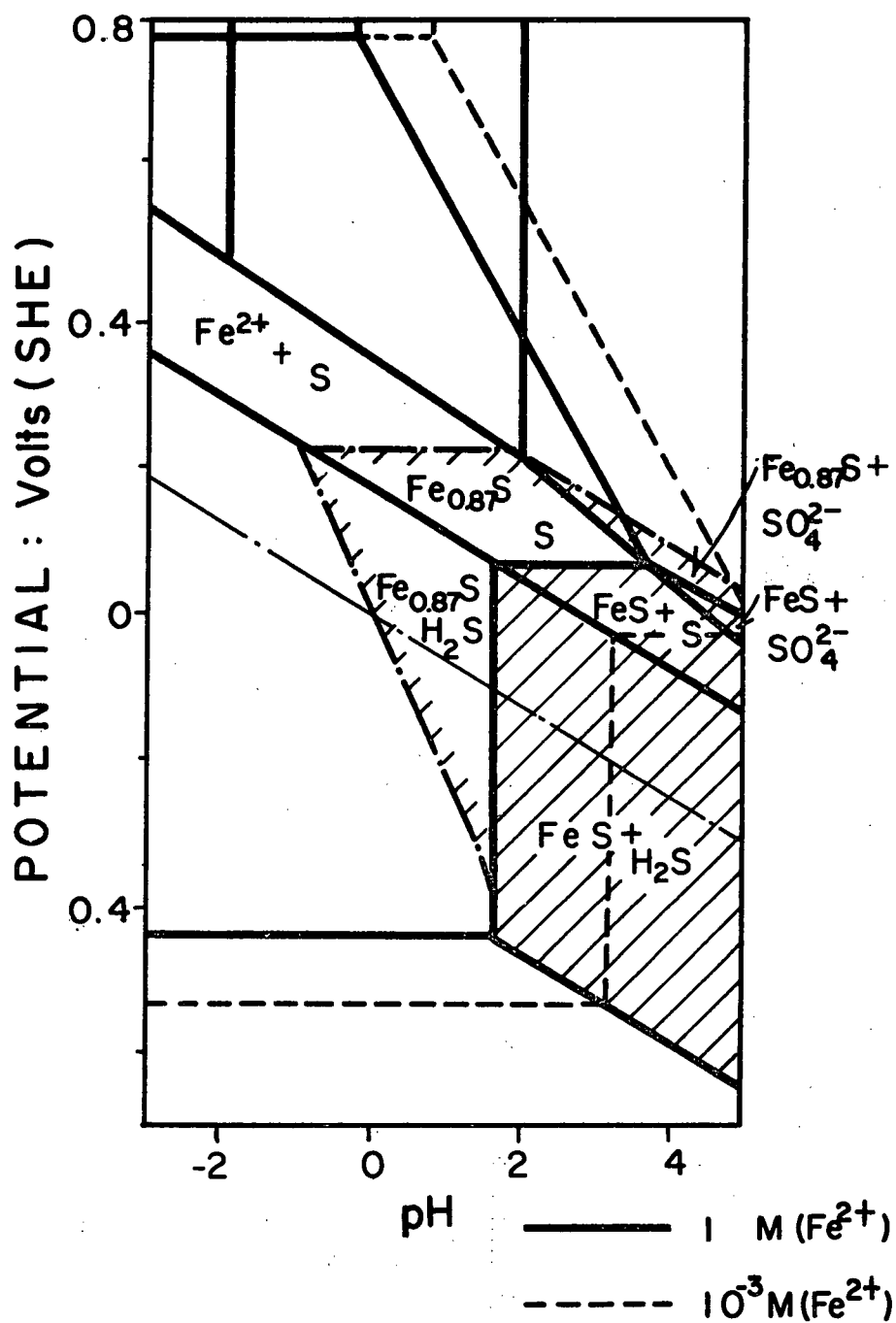
Figure 5. Potential-pH diagram for metastable Fe-S systems at 25°C under conditions where pyrite is not formed.

of this non-stoichiometric compound. The composition $Fe_{0.87}S$ is near that which corresponds to equilibrium with pyrite, i.e., monoclinic pyrrhotite, Fe_7S_8.

(2) Electrochemical Study of Pyrrhotite

An early electrochemical study in pyrrhotite was made by K.E. Wrabetz,[5] as a part of extensive contributions to electrochemical studies of sulphides by both himself and his co-workers. In this study the synthesized pyrrhotite was used to investigate the effect of ferrous ion concentration on the electrode potential. The data are shown in Table I.

Table I. Measured potential of the cell $(-)FeS/FeSO_4 \cdot XM/KCl/Calomel$ R.E.$(+)$ at 18°C.

$[Fe^{++}]$ M	E (mV) vs S.H.E.	$[Fe^{++}]$ M	E (mV) vs S.H.E.
0.358	396	0.0075	394
0.138	387	0.0020	402
0.042	394	0.00046	399
0.020	406	\<average\>	397

As seen in Table I, it was concluded that the potential did not depend on ferrous ion concentration in range of 0.0004 ∿ 0.3 M. Further, using the cell $(-)FeS/FeSO_4$, 0.1 M. H_2SO_4, 0.1 M/KCl/Calomel R.E. $(+)$ the potential measured showed -0.40 ∿ -0.45 V(S.H.E.) for the synthesized

pyrrhotite and +0.51 V(S.H.E.) for the natural pyrrhotite. There was

a large difference in potential between those pyrrhotites. This

difference in potential was not interpreted in his work.

Then, M. Sato[6] published a systematic work in several sulphides

that was undertaken to measure the rest potential of sulphides in

changing the pH, and the concentrations of corresponding metal ions and

sulphide ions in the electrolyte. Unfortunately the potential

measurement of pyrrhotite in the acid region failed because of its

poor reproducibility caused by the formation of hydrogen sulphide

and ferrous ions through the action of acids. Nevertheless, the data

in basic regions showed that the potential for the natural pyrrhotite

was about 600 mV higher than that for the synthesized pyrrhotite.

Recently S. Venkatachalam and R. Mallikarjunan[7] showed the

independence of the potential of the precipitated ferrous sulphide on

ferrous ion concentration in the range of 0.001 ∿ 0.5 M in ferrous

ammonium sulphate solution.

For the general electrochemical behaviour of pyrrhotite in acid

regions it can be described that the rest potential is not influenced

by ferrous ion concentration in the electrolyte and the rest potential

of natural pyrrhotite is more noble than that of synthesized pyrrhotite.

(3) Leaching of Pyrrhotite

It is well known that pyrrhotite easily dissolves into acid

solution forming ferrous ions and hydrogen sulphide as reaction products

according to the following equation,

$$FeS + 2H^+ \rightleftharpoons Fe^{++} + H_2S \ (\uparrow) \qquad (III-1)$$
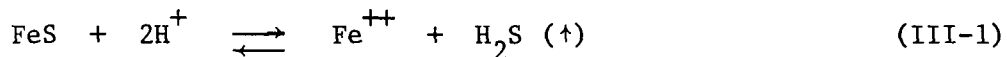
This occurs in Kipp's generators to produce hydrogen sulphide in standard chemical laboratories.

H.A. Pohl[8] proposed the following mechanism of hydrogen sulphide evolution from the precipitated ferrous sulphide in acid,

$$FeS + H^+ \longrightarrow Fe^{++} + HS^- \qquad (III-2)$$

$$HS^- + H^+ \longrightarrow H_2S \ (\uparrow) \qquad (III-3)$$
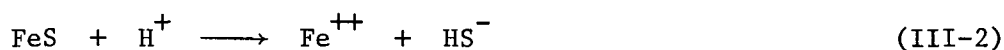
accounting for the fact that FeS, CdS and ZnS dissolve in kinetically first order reactions with respect to the concentration of hydrogen ion, which suggests the step of (III-2) as a rate-determining reaction.

In industry the hydrogen sulphide formed from pyrrhotite can be of interest to produce elemental sulphur as a commercially valuable product by the oxidation process, i.e.

$$H_2S + 1/2O_2 \longrightarrow H_2O + S^o \qquad (III-4)$$
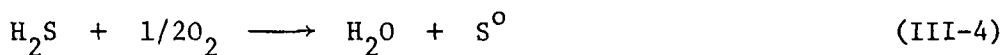
When pyrrhotite is directly oxidized in aqueous media by oxygen, the following stoichiometry of reaction is established,

$$4FeS + 3O_2 \longrightarrow 2Fe_2O_3 + 4S \qquad (III-5)$$
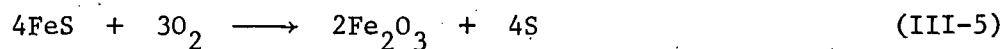
The mechanism of the oxidation process of pyrrhotite is not fully

understood yet.

K.W. Downes and R.W. Bruce[9] carried out the oxidation of pyrrhotite

at 110-125°C under high oxygen pressure. In autoclave experiments

no elemental sulphur was observed except when the pH of the solution

reached about 1.5. The evolution of hydrogen sulphide, when pyrrhotite

is added to autoclave liquor at room temperature, has been noticed.

These facts lead to the postulation of the following mechanism of

reaction; water and pyrrhotite in the autoclave react first forming

ferrous sulphate,

$$FeS + 2O_2 \longrightarrow FeSO_4 \qquad\qquad (III-6)$$

This sulphate is oxidized to ferric sulphate,

$$6FeSO_4 + 1 \ 1/2O_2 \longrightarrow 2Fe_2(SO_4)_3 + Fe_2O_3 \qquad (III-7)$$
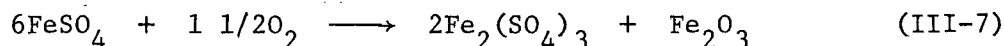
This ferric sulphate being unstable in neutral water hydrolyses to

ferric oxide and sulphuric acid,

$$Fe_2(SO_4)_3 + 3H_2O \longrightarrow Fe_2O_3 + 3H_2SO_4 \qquad (III-8)$$
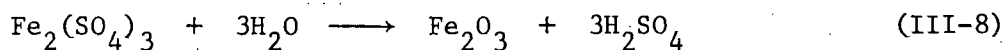
The sulphuric acid then dissolves pyrrhotite to form H_2S and ferrous

sulphate,

$$FeS + H_2SO_4 \longrightarrow FeSO_4 + H_2S \qquad\qquad (III-9)$$
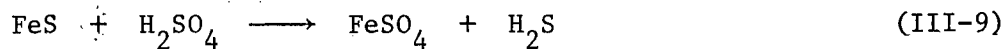
As a following step, H_2S is oxidized by ferric sulphate or oxygen to form elemental sulphur,

$$H_2S + Fe_2(SO_4)_3 \longrightarrow 2FeSO_4 + H_2SO_4 + S^o \qquad \text{(III-10)}$$

$$H_2S + 1/2O_2 \longrightarrow H_2O + S^o \qquad \text{(III-4)}$$
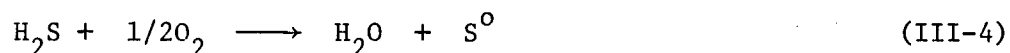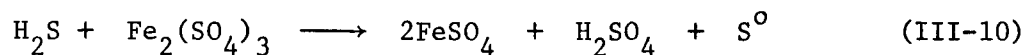
J. Gerlach, H. Hahne and F. Pawlek[10] studied the kinetics of the oxygen pressure leaching of pyrrhotite. Sulphur, hydrogen sulphide and sulphate were detected as reaction products of sulphur during leaching, then, as a mechanism of reaction the following steps were proposed.

$$FeS + 2H^+ \rightleftharpoons H_2S + Fe^{++} \qquad \text{(III-1)}$$

$$H_2S + 1/2O_2 \longrightarrow S^o + H_2O \qquad \text{(III-4)}$$

$$H_2S + 2O_2 \longrightarrow SO_4^{=} + 2H^+ \qquad \text{(III-11)}$$

$$H_2S + 2Fe^{+++} \longrightarrow S^o + 2Fe^{++} + 2H^+ \qquad \text{(III-12)}$$

$$H_2S + 8Fe^{+++} + 4H_2O \longrightarrow SO_4^{=} + 8Fe^{++} + 10H^+ \qquad \text{(III-13)}$$
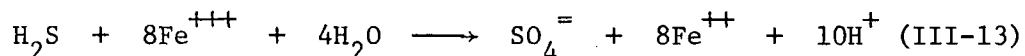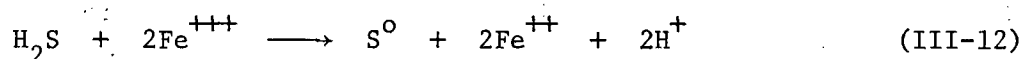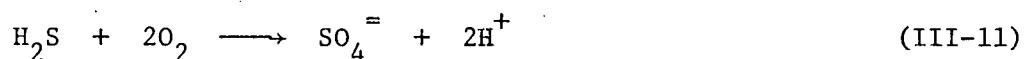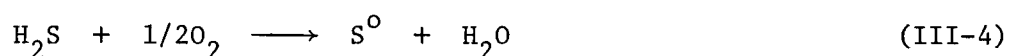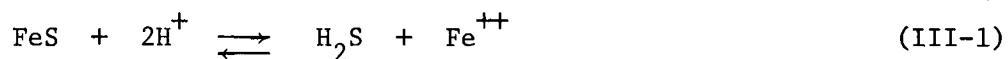
Also, elemental sulphur reacts with oxygen to form sulphate ion,

$$S^o + 3/2O_2 + H_2O \longrightarrow SO_4^{=} + 2H^+ \qquad \text{(III-14)}$$
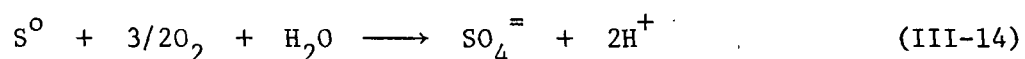
The oxidation of ferrous to ferric ion by oxygen occurs relatively slowly in sulphuric acid media, so the reactions (III-12) and (III-13) seem less significant, but the reaction (III-1) is predominant because most of the sulphur was found as elemental sulphur (more than 70%).

IV. THE METAL SULPHIDE ELECTRODE

(1) Thermodynamic Aspect

A metal sulphide electrode consists of two components and therefore its equilibrium potential can be described in terms of either of its components, i.e. according to the Nernst equation for equilibrium between metal in the sulphide and metal cation in the electrolyte,

$$M^{+n}_{(aq)} \quad + \quad ne \quad \rightleftarrows \quad M^{O} \text{ (in sulphide)}$$

$$E_M = E_M^O + \frac{2.3RT}{nF} \log \frac{a_{M^{n+}}}{a_{M^O}} \tag{IV-1}$$
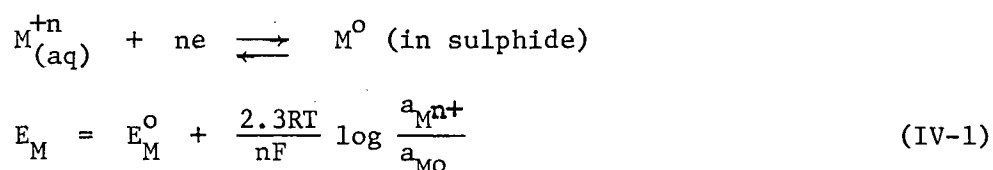
and for equilibrium between sulphur in the sulphide and hydrogen sulphide,

$$S^{O} \text{ (in sulphide)} \quad + \quad 2H^{+} \quad + \quad 2e \quad \rightleftarrows \quad H_2S \text{ (aq)}$$

$$E_S = E_S^O + \frac{2.3RT}{2F} \log \frac{a^2_{H^+} \cdot a_{S^O}}{a_{H_2S}} \tag{IV-2}$$
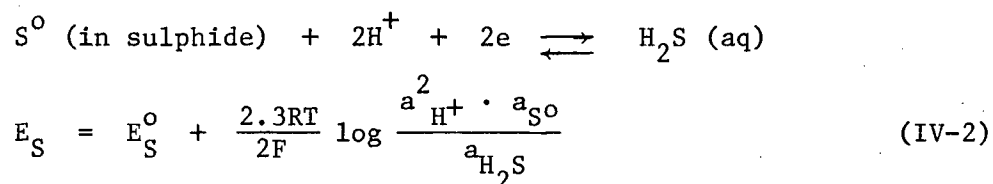
where E_M^O and E_S^O are the standard electrode potentials.

When equilibrium is reached between the electrode and the electrolyte, i.e. the sulphide is in a total solubility equilibrium with the electrolyte, the value of the potential is the same in both cases, because the electrode can exert only one potential. Therefore, according to equations (IV-1) and (IV-2),

$$E = E_M^o + \frac{2.3RT}{nF} \log \frac{a_{M^{n+}}}{a_{MO}} = E_S^o + \frac{2.3RT}{2F} \log \frac{a_{H^+}^2 \cdot a_{S^o}}{a_{H_2S}} \qquad \text{(IV-3)}$$

is obtained.

A basic thermodynamic property of the metal sulphide, $M_{2/n}S_{1+\alpha}$ ($\alpha \ll 1$), is that the free enthalpy of formation of the sulphide phase defines the relationship between metal and sulphur activities, i.e.

$$2/nM^o + (1+\alpha)S^o \;\underset{\longleftarrow}{\longrightarrow}\; M_{2/n}S_{1+\alpha} \qquad \text{(IV-4)}$$
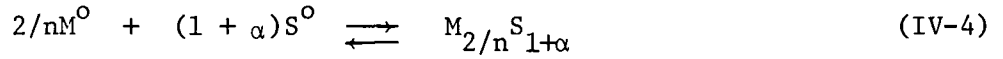
$$\Delta F_{(4)}^o = -2.3RT \log[a_{M_{2/n}S_{1+\alpha}} / a_{MO}^{2/n} \cdot a_{S^o}^{(1+\alpha)}]$$

$$= 2.3RT \log a_{MO}^{2/n} \cdot a_{S^o}^{(1+\alpha)} \qquad \text{(IV-5)}$$

where $a_{M_{2/n}S_{1+\alpha}} = 1$

For a solubility equilibrium

$$M_{2/n}S_{1+\alpha} + 2H^+ \;\underset{\longleftarrow}{\longrightarrow}\; 2/nM^{n+} + H_2S + \alpha S^o \qquad \text{(IV-6)}$$
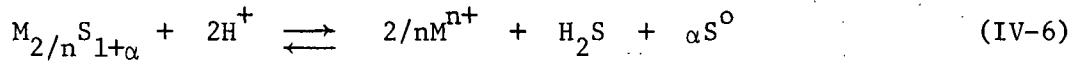
$$K_{(6)} = \frac{a_{M^{n+}}^{2/n} \cdot a_{H_2S} \cdot a_{S^o}^{\alpha}}{a_{M_{2/n}S_{1+\alpha}} \cdot a_{H^+}^2} = \frac{a_{M^{n+}}^{2/n} \cdot a_{H_2S} \cdot a_{S^o}^{\alpha}}{a_{H^+}^2} \qquad \text{(IV-7)}$$

is obtained, where $K_{(6)}$ is the equilibrium constant for (IV-6) and $a_{M_{2/n}S_{1+\alpha}} = 1$ as mentioned before. According to (IV-2) and (IV-7), the following equation can be obtained:

$$E_S = E_S^o + \frac{2.3RT}{2F} \log [a_{M^{n+}}^{2/n} \cdot a_{S^o}^{1+\alpha} / K_{(6)}] \qquad \text{(IV-8)}$$

From this equation and (IV-5)

$$E_s = E_S^o - \frac{2.3RT}{2F} \log K_{(6)} + \frac{2.3RT}{2F} \log a_{M^{n+}}^{2/n} + \frac{1}{2F}(F_{(4)}^o - 2.3RT \log a_{M^o}^{2/n})$$

$$= E_S^o - \frac{2.3RT}{2F} \log K_{(6)} + \frac{\Delta F_{(4)}^o}{2F} + \frac{2.3RT}{2F} \log a_{M^{n+}}^{2/n} - \frac{2.3RT}{2F} \log a_{M^o}^{2/n}$$

$$= E_S^o - \frac{2.3RT}{2F} \log K_{(6)} + \frac{\Delta F_{(4)}^o}{2F} + \frac{2.3RT}{nF} \log(a_{M^{n+}}/a_{M^o}) \qquad (IV-9)$$

is obtained. In (IV-9)

$$E_S^o - \frac{2.3RT}{2F} \log K_{(6)} + \frac{\Delta F_{(4)}^o}{2F} = E_M^o$$

therefore,

$$E_S = E_M^o + \frac{2.3RT}{nF} \log \frac{a_{M^{n+}}}{a_{M^o}}$$

This equation shows the validity of (IV-3).

(2) Kinetic Aspect

The reversible potential of sulphide electrodes which can be calculated from thermochemical data using the Nernst equation does not always agree with that obtained in measurements. This arises because most sulphide electrode systems belong to a polyelectrode system where a kinetic consideration is necessary to interpret the potential of the sulphide electrode. In the acid region the possible electrochemical reactions in this polyelectrode system include;

1. Oxidation of metal in the sulphide to metal cations

$$M^o(\text{in sulphide}) \longrightarrow M^{n+} + ne; \qquad\qquad i_{a1}$$
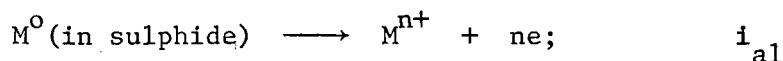
2. Oxidation of sulphur in the sulphide to sulphate ions,

$$S^O \text{ (in sulphide)} + 4H_2O \longrightarrow SO_4^= + 8H^+ + 6e; \quad i_{a2}$$
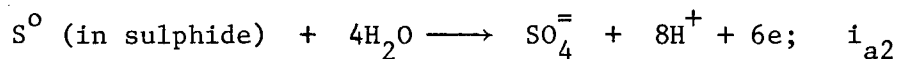
3. Reduction of sulphur in the sulphide to hydrogen sulphide,

$$S^O \text{ (in sulphide)} + 2H^+ + 2e \longrightarrow H_2S; \quad i_{c3}$$
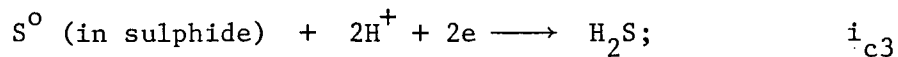
4. Reduction of hydrogen ions into hydrogen molecules,

$$2H^+ + 2e \longrightarrow H_2; \quad i_{c4}$$

5. Reduction of corresponding metal ions, which are added to electrolyte, into metal,

$$M^{n+} + 2e \longrightarrow M^O; \quad i_{c5}$$
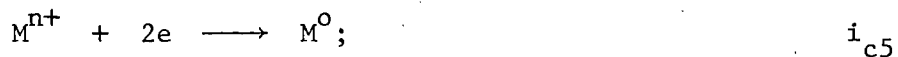
6. Oxidation of hydrogen sulphide which is dissolved in the electrolyte, into elemental sulphur,

$$H_2S \longrightarrow S^O + 2H^+ + 2e; \quad i_{a6}$$
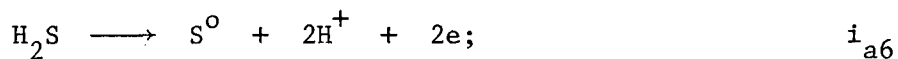
These reduction and oxidation, i.e. cathodic and anodic processes can occur simultaneously but statistically independent of one another.

The rate of each reaction, i.e. current density, i_c or i_a, can be described by the following equations, according to electrochemical kinetics.[11,12]

Table IV.   Equilibrium constants of $M_{2/n}S + 2H^+ = H_2S(aq) + 2/nM^{n+}$

for various sulphides at 25°C

$$K = a_{M^{n+}}^{2/n} \cdot a_{H_2S}/a_{H^+}^2$$

Sulphide	log K	Sulphide	log K
MnS	8.0	CdS	- 6.14
FeS	2.55	PbS	- 7.10
CoS	-0.33	CuS	-15.0
NiS (γ)	-6.69	Cu_2S	-18.9
ZnS (Spal)	-4.12	Ag_2S	-15.58
(Wurt)	-1.80	HgS	-32.3

According to this equation, although $a_{H_2S(aq)}$ is dependent on $a_{Fe^{++}}$

in the case when $a_{Fe^{++}}$ is 10^{-2} or less than it, the activity of

aqueous hydrogen sulphide at equilibrium is more than 3.55×10^{-2}

which suggests the continuous evolution of hydrogen sulphide into the

He gas atmosphere which is used in this work. On the other hand,

Table IV states that CuS, Cu_2S, Ag_2S and PbS have extremely small

values of K. This is associated with negligible H_2S evolution and

therefore promises the possibility of measuring the reversible potential

of the respective sulphides, and indeed these have been experimentally

obtained.[6,16]

When the rest potential of pyrrhotite is controlled by the reactions

of [Fe] $\rightarrow Fe^{++} + 2e$ as an anodic process and [S] $+ 2H^+ + 2e \rightarrow H_2S$

as a cathodic process, the current density of each reaction can be

equated according to Equations (IV-10) and (IV-11); for the anodic process

for anodic current density,

$$i_a = ZFk_a \; a_1^m \cdot a_2^n \ldots a_p^r \; \exp \{\frac{Z\alpha.F}{RT} \varepsilon\}$$ (IV-10)

for cathodic current density,

$$i_c = -ZFk_c \; a_1^u \cdot a_2^v \ldots a_q^w \; \exp \{\frac{-Z\beta F}{RT} \varepsilon\}$$ (IV-11)

where k_a, k_c are reaction rate constants for anodic and cathodic reactions, respectively; a_p, a_q are activities of reactants of anodic and cathodic reactions, respectively; m, n, r, u, v, w, are orders of anodic and cathodic reactions with respect to each reactant; Z is the number of electrons involved in each reaction; α, β are transfer coefficients for anodic and cathodic reactions, respectively; F is the Faraday constant; and ε is the potential of the sulphide electrode. According to these equations, the rate of each reaction will be governed by the electrical potential at the sulphide electrode, rate constant, activities of reactants and the transfer coefficient. If a steady state is established and there is no external disturbance, the sum of cathodic reaction rates will be equal to the sum of anodic reaction rates;

$$\Sigma i_c = \Sigma i_a$$ (IV-12)

Considering the topography of the electrode surface in the poly-electrode system, it is not necessary to have separate macroscopic areas

which are exclusively cathodic or anodic on a sulphide electrode,
either operationally or conceptually. Any one site may be anodic
during one instant of time and cathodic during another instant, and
anodic and cathodic processes can occur simultaneously on atomically
adjacent sites. This homogeneous surface condition will become
especially important when we consider current density instead of
current in a quantitative understanding of the electrochemical
behaviour of the electrode.

Here, it is helpful to use a current-density potential diagram
in order to understand better the current-density potential relationship
in the polyelectrode system. In Fig. 6 the possible reactions, 1)-6)
are schematically plotted. The locations of each line depends on the
parameters such as k_a, k_c, a_p, a_q. Also the slope of each line depends
on the value of α or β and Z. The effect of concentration polarization
which will be significant at high current-density in this diagram
is not accounted for in order to simplify the discussion. In this
sulphide polyelectrode system where each possible reaction is independent
and alternative, the potential of the electrode is largely determined by
the coupled reactions which have the highest current-density. The
highest possible current densities, i_{01} and i_{02} are shown in Fig. 6,
as the intersections of cathodic and anodic lines coordinated with the
potentials of the electrode E_{01} and E_{02}. Strictly speaking, this
interpretation for the potential from the intersection of both lines
is not correct, because equation (IV-12) can not be satisfied at the
intersection. However, if the other minute current densities at the
potential E_{01} or E_{02} were neglected, equation (IV-12) yields
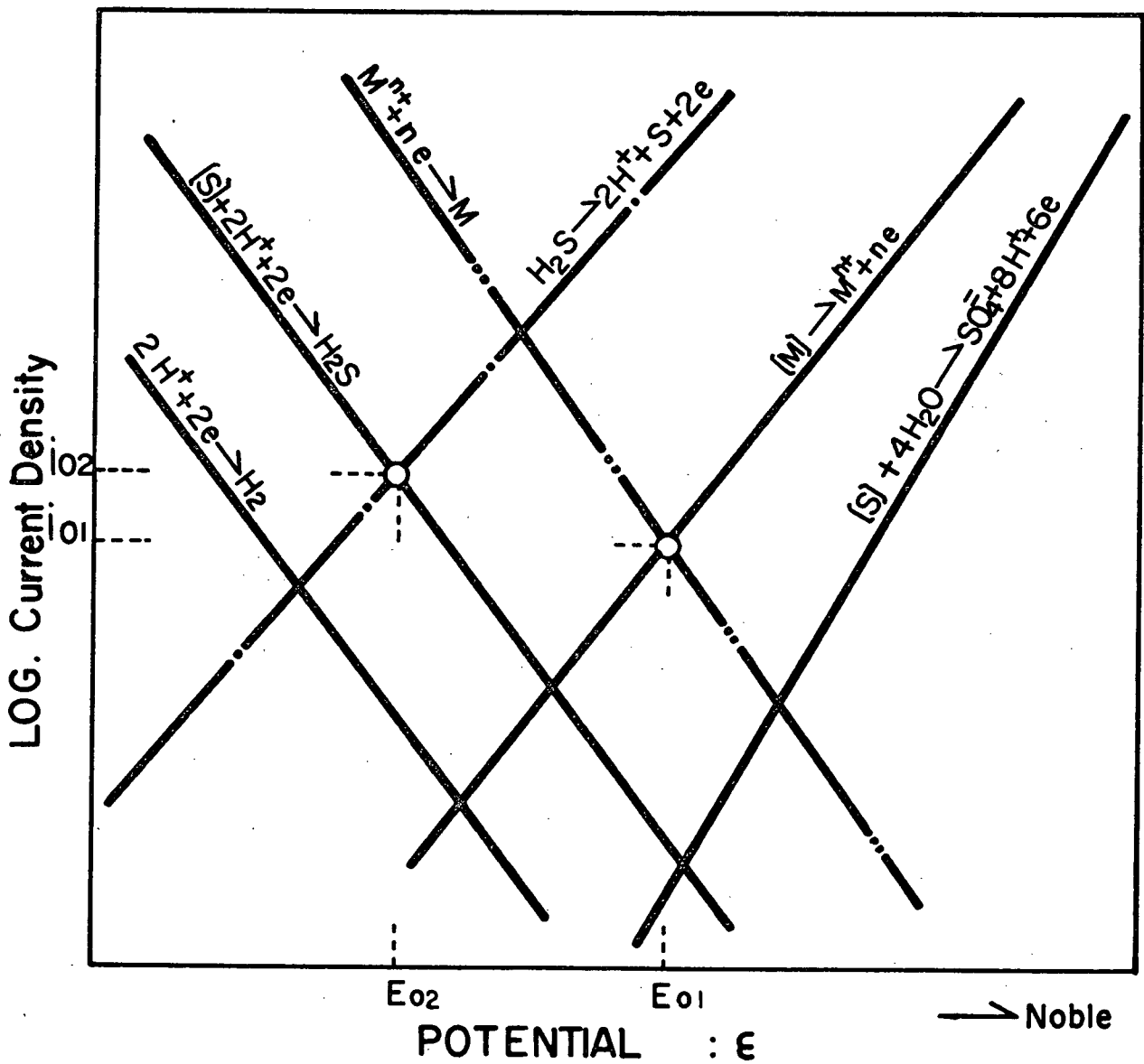
Figure 6. Schematic diagram for current-density potential relationships of sulphide electrode in acid region.

$$i_a = i_c \tag{IV-13}$$

When both of the coupled reactions determining the potential of the sulphide are identical, as the example shown in Fig. 6, the potential is called the reversible or equilibrium potential. In either of these cases, the reversible potential for the metal–metal cation equilibrium, from (IV-10), (IV-11), (IV-13) and $Z = n$

$$i_{01} = i_a = -i_c = nFk_a\, a_{M^0}\, \exp\left\{\frac{n\alpha F}{RT}\, E_{01}\right\} = nFk_c\, a_{M^{n+}}\, \exp\left\{-\frac{n\beta F}{RT}\, E_{01}\right\} \tag{IV-14}$$

is obtained. Equation (IV-14) yields

$$E_{01} = \frac{RT}{(\alpha+\beta)nF}\, \ell n\, \frac{k_c}{k_a} \cdot \frac{a_{M^{n+}}}{a_{M^0}}$$

Here, $\alpha+\beta = 1$ in the case when anodic and cathodic processes are identical and $k_c/k_a = K$ which is the equilibrium constant for $M^{n+} +$ ne $\rightleftarrows$ M^0. Therefore,

$$E_{01} = \frac{RT}{nF}\, \ell n\, K + \frac{RT}{nF}\, \ell n\, \frac{a_{M^{n+}}}{a_{M^0}}$$

$$= E_M^0 + \frac{2.3RT}{nF}\, \log\, \frac{a_{M^{n+}}}{a_{M^0}} \tag{IV-15}$$

This equation is identical with the Nernst equation derived in the section on thermodynamic considerations. In the same manner for the sulphur–hydrogen sulphide equilibrium the reversible potential

$$E_{02} = E_S^o + \frac{2.3RT}{2F} \log \frac{a_{S^o} \cdot a_{H^+}^2}{a_{H_2S}} \qquad \text{(IV-16)}$$

is derived.

V. EXPERIMENTAL

(1) Materials

Natural and synthesized pyrrhotites were used in this experiment.

Natural minerals were obtained from the Sullivan Mine in Kimberley, B.C.

and the Chichibu Mine in Japan. Microscopic observations did not show

any other phase except pyrrhotite. Natural pyrrhotites are in a more

stable state thermodynamically than synthesized pyrrhotites. However,

they invariably contain impurity elements such as Ni, Co, Cu, As etc.

For experimental purposes it is very difficult to obtain pyrrhotites

having a systematically varying range of composition. The synthesized

pyrrhotites are required especially to examine the Fe:S composition

ratio. Three methods were used in this work to synthesize pyrrhotites.

Method I.

Sulphur lump crystals (chemical pure) and iron wire (99.9%,

0.022 cm diameter) respectively were weighed out to correspond to an

appropriate composition of pyrrhotite, then placed together into a 96%

silica glass ("Vycor") tube, 0.8 cm outer-diameter, which was

evacuated and sealed. The Vycor tube was placed in the furnace,

heated to 500°C for one day and to 700°C for two days, then furnace

cooled to room temperature. In each Vycor tube about one gram pyrrhotite

was produced. At 700°C the sulphur decomposition pressure equilibrated

with pyrrhotite was negligibly small up to the composition of the
pyrrhotite of 48 atomic percent Fe, i.e. less than 0.1 atm, so it was
assumed that all sulphur put into the Vycor tube reacted with iron.
However, below about 48 atomic percent Fe the sulphur decomposition
pressure of pyrrhotite can not be neglected in the material balance of
sulphur. Therefore this method was not used for preparing pyrrhotite
material of less than 48 atomic percent Fe.

Method II.

The "Dew point method"; the apparatus for this method consisted of
a Vycor tube, 1.5 cm outer-diameter and 30 cm length, in which sheet
iron (99.99%) and sulphur were placed at each end, then this tube was
evacuated, sealed and placed in furnace system which consists of
two separately heated zones. On the iron side the temperature was
kept constant at 700°C, while on the sulphur side the temperature was
adjusted in the range 110°C to 450°C to establish a chosen partial
pressure of sulphur. In this method, by weighing the iron samples
before and after each run the iron content in sulphide can be calculated.
Thus the determination of Fe content in the pyrrhotite does not contain
any error due to incomplete reaction of sulphur. However, when the iron
being sulphidized was kept at 700°C, a sulphur temperature between 110°C
to 450°C was too high to synthesize the pyrrhotite containing more
than 48 atomic percent Fe. Thus methods I and II in combination permitted
the synthesis of pyrrhotites with wide range of composition.

In this method each run took 4 days to complete sulphidization of
sheet iron (0.04 cm thickness) and to homogenize the resulting pyrrhotite.

The vapour pressure of sulphur is known from the work of W. West and A. Menzies,[13] shown in Fig. 7. It was assumed that by steady state conditions the total sulphur pressures at both ends in the Vycor tube were equal but not the partial pressures of the different molecular species. The vapour density of the gas increased markedly from the hot zone at 700°C, where the gas consisted of mainly S_2 molecules, to the colder part held in the range 110-450°C, where it consisted of S_8, S_7, S_6, S_5, S_4, S_3 and S_2 molecules. In Fig. 8 the variation in Fe content with different sulphur bath temperatures is shown. Pyrrhotite made at 700°C was fairly massive and could be used for electrodes in electrochemical studies.

Method III.

This method can be called the "Melt method". Iron powder, 99% purity, and sulphur powder were mixed in a weight ratio of 1:1; then this mixture was gradually heated in a graphite crucible to 700°C at which temperature it was held for 5 hours. After that the temperature was increased to 1250°C, above the melting point (1190°C) of FeS, where molten FeS was kept for a half an hour, then cooled to 750°C, from this temperature the sample was cooled to room temperature over a period of 10 days. All processes of heating, melting and cooling were undertaken in an inert atmosphere of He flow. This pyrrhotite was supposed to be iron saturated or less excess sulphur pyrrhotite. This technique was essential for the production of lumps of pyrrhotite.

Besides pyrrhotites, other materials occasionally used were pyrite, iron powder and chalcocite. The source of pyrite was not known, chalcocite was from Montana, U.S.A. Iron powder used was of 99% purity.
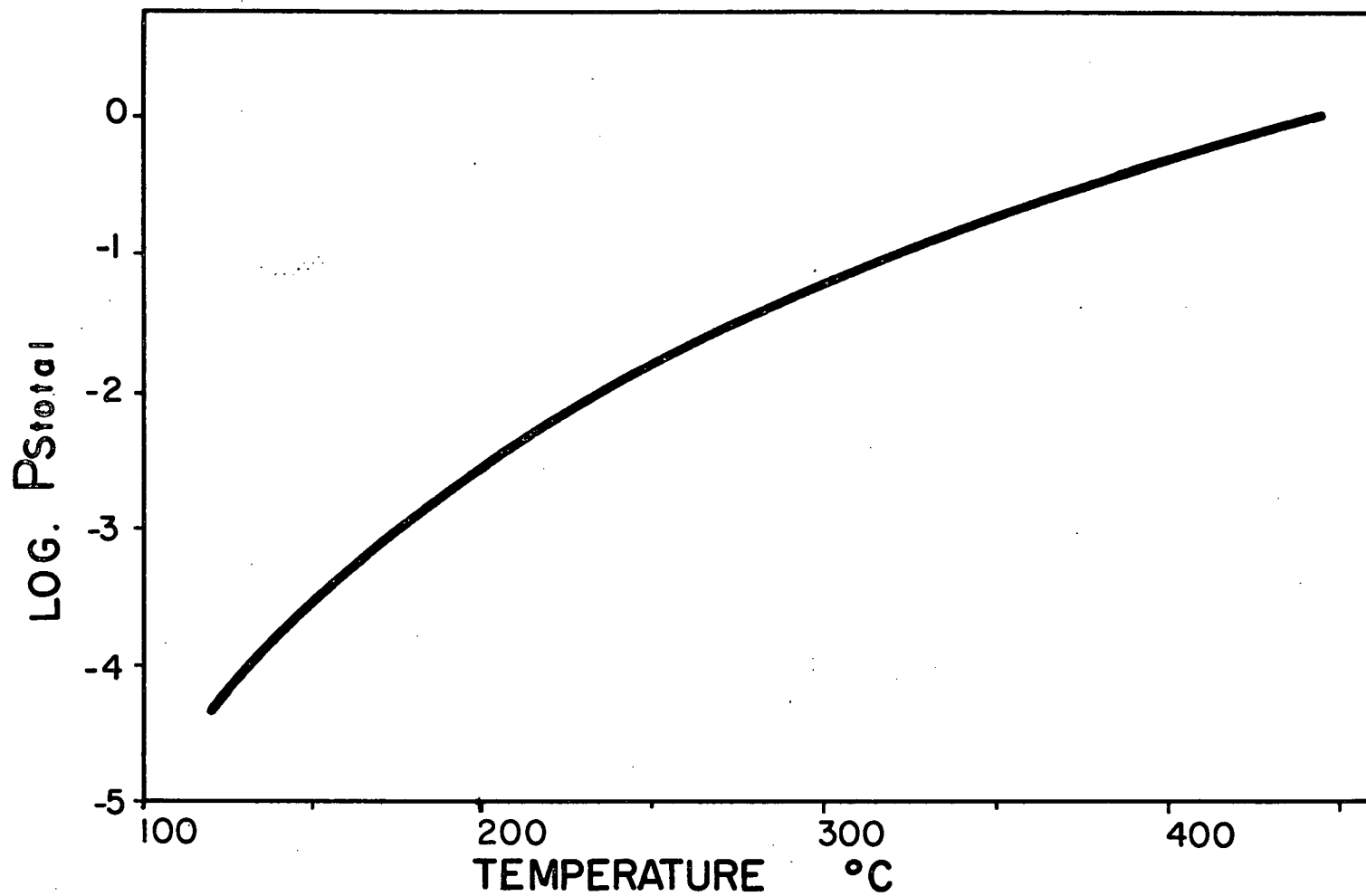
Figure 7. Total vapour pressure of sulphur between 120 and 450°C.
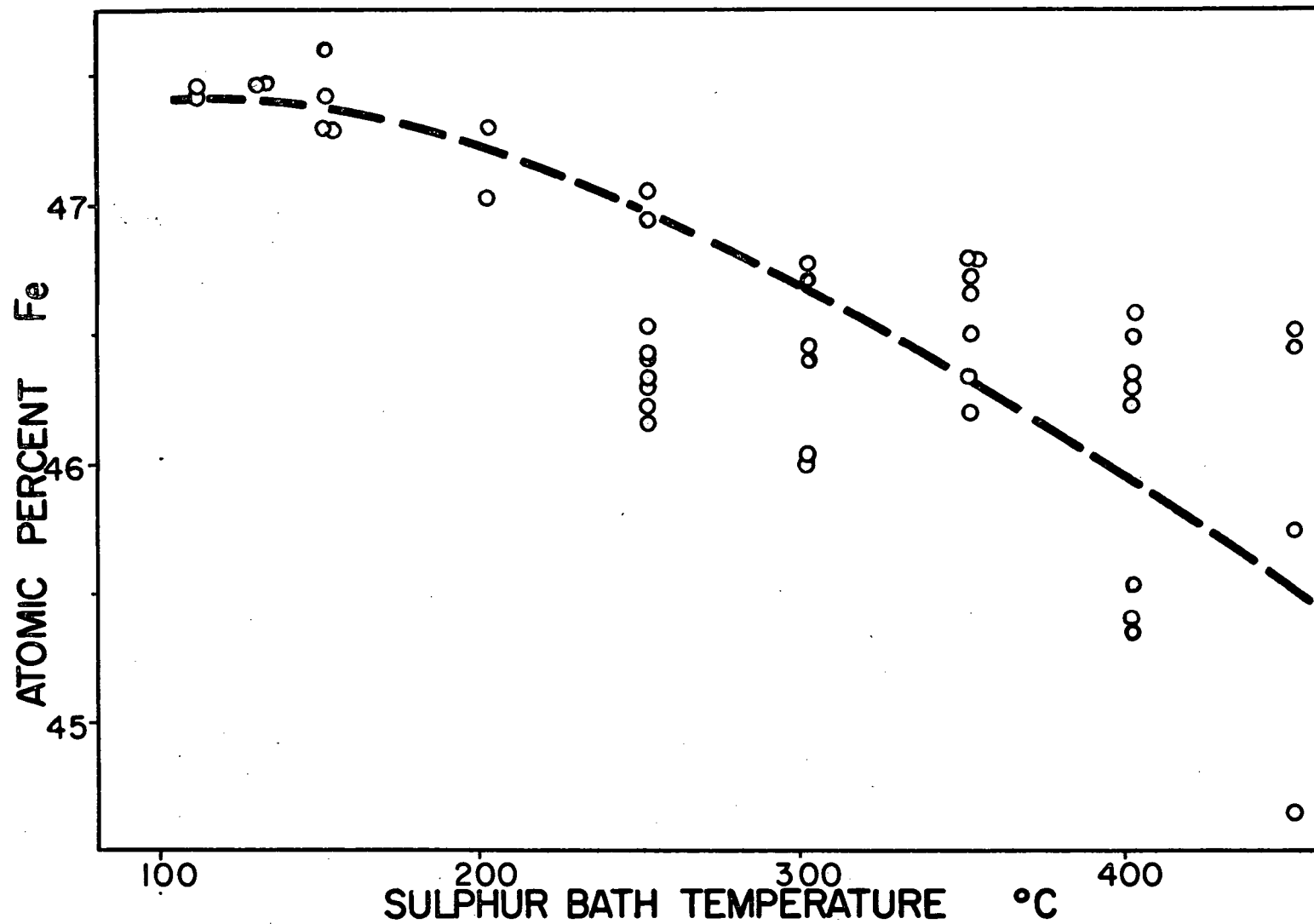
Figure 8. Variation in Fe content with different sulphur bath temperatures.

(2) <u>X-Ray Analysis of Pyrrhotites</u>

Pyrrhotites used in this study were examined by X-ray diffraction

to identify the phases present. A Debye-Scherrer camera was used to

take the powder diffraction patterns with a CoK_α X-ray tube. In Fig. 9

the X-ray diffraction patterns are presented. ASTM cards for pyrrhotite,

pyrite, and marcasite are included on lines 1, 10 and 11, respectively

for comparison with results obtained. According to these data, it can

be concluded that pyrrhotites synthesized by methods described

corresponded to pyrrhotite, while neither pyrite nor marcasite were

present. The diffraction line represented by (102), which has the

highest intensity, changed slightly in position due to the extent

of non-stoichiometry of pyrrhotite as reported by M. Haraldsen.[14]

However, data obtained in this work were too scattered to establish a

reliable relationship. In patterns 12 and 13, the powder pyrrhotites

before and after the rest potential measurement were examined to check

the possibility of a phase change; however, X-ray pictures indicated

that no such phase change occurred, because both X-ray patterns were

essentially identical. The phase relationships described earlier was

not apparent in this X-ray study.

(3) <u>Sulphide Electrodes</u>

In this study two kinds of sulphide electrodes were used. One of

them was made in the following way; a mineral plaque was mounted in self-

setting plastic resin, "Koldmount", with the two flat sides free from

resin. A mercury contacting column containing a copper lead wire was

formed in a resin mount on one of the free sides of the electrode, which
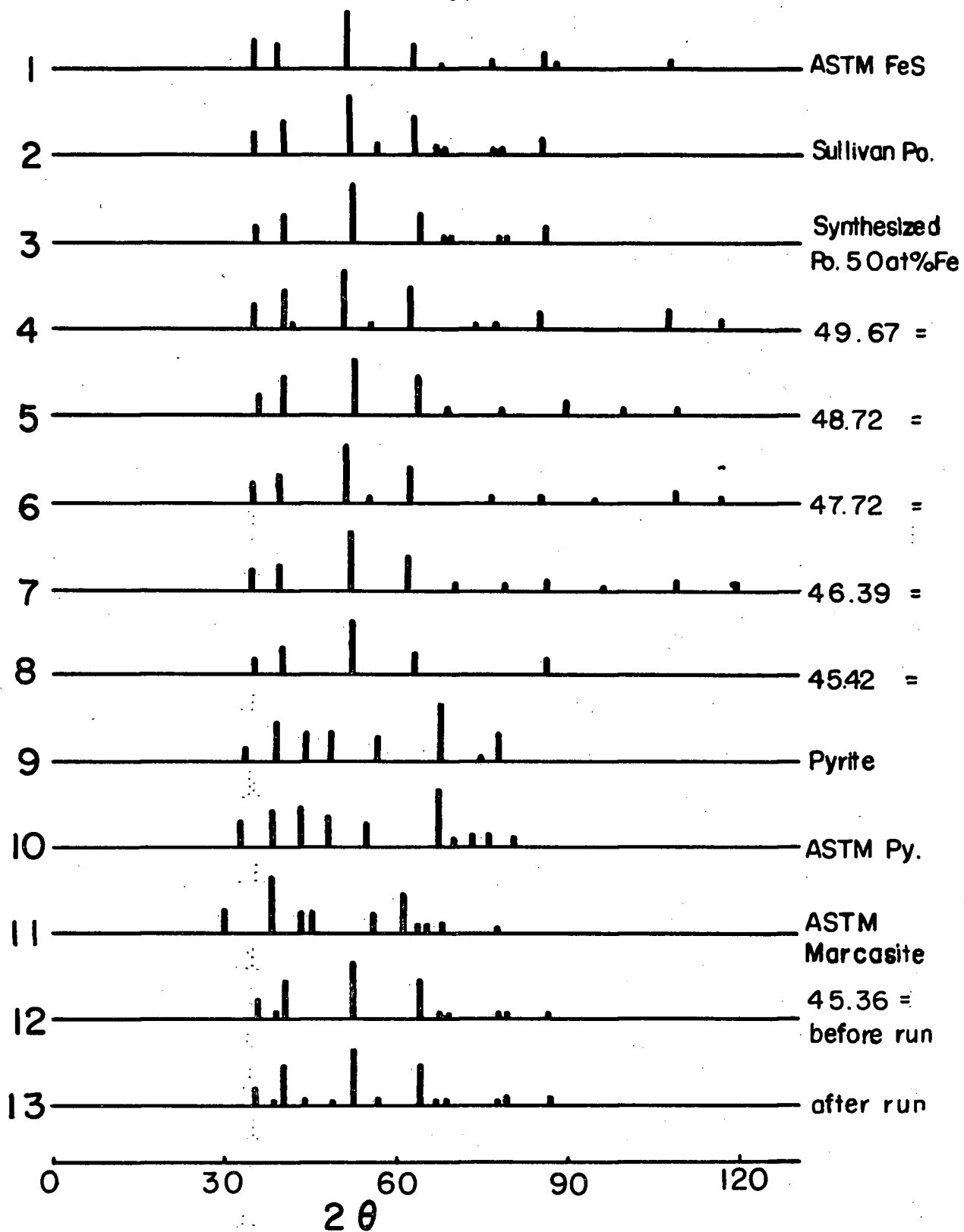
Figure 9. X-ray diffraction patterns of various iron sulphides using Co-K$_\alpha$ radiation.

remained isolated from the solution. The other free side then became the active electrode surface in contact with the electrolyte. A drawing of this "mounted electrode" is shown in Fig. 10(a).

The other electrode consisted of sulphide powder floating on a mercury pool. A glass U-tube was filled with mercury on one side of which the sulphide powder was floated. A copper lead wire entered the mercury from the other side for an electrical connection. This electrode, called a "powder electrode", is shown in Fig. 10(b). Mercury is known as a thermodynamically noble metal whose standard single electrode potential is +0.789 volts and has a very high hydrogen overvoltage associated with a very low exchange current density, $i_o = 10^{-13}\text{-}10^{-11}$ A/cm^2.[15] In addition, pyrrhotite will not react with mercury because of more negative standard free enthalpy of formation of sulphides for FeS, -23.32 Kcal/mole, than that for HgS, -11.05 Kcal/mole. These factors were considered in the experiments comparing the rest potentials when measured with the mounted electrodes as compared to the powder electrode. In Table II the results for both natural pyrrhotite and chalcocite are shown.

Table II. Comparison of the rest potential measured with the mounted electrode and the powder electrode.

Chichibu pyrrhotite, 25°C pH = 2.85, $[Fe^{++}]$ = 0.01 M	Chalcocite, 25°C pH = 1.35 $[Cu^{++}]$ = 0.1 M
mounted electrode	mounted electrode
+161 mV (S.H.E.) +143	+433 mV (S.H.E.)
powder electrode	powder electrode
+186 mV (S.H.E.) +124	+439 mΔ (S.H.E.)

Copper
lead wire

Glass tube

Mercury

Resin

Sulphide

(a)

Sulphide
powder

Mercury

(b)
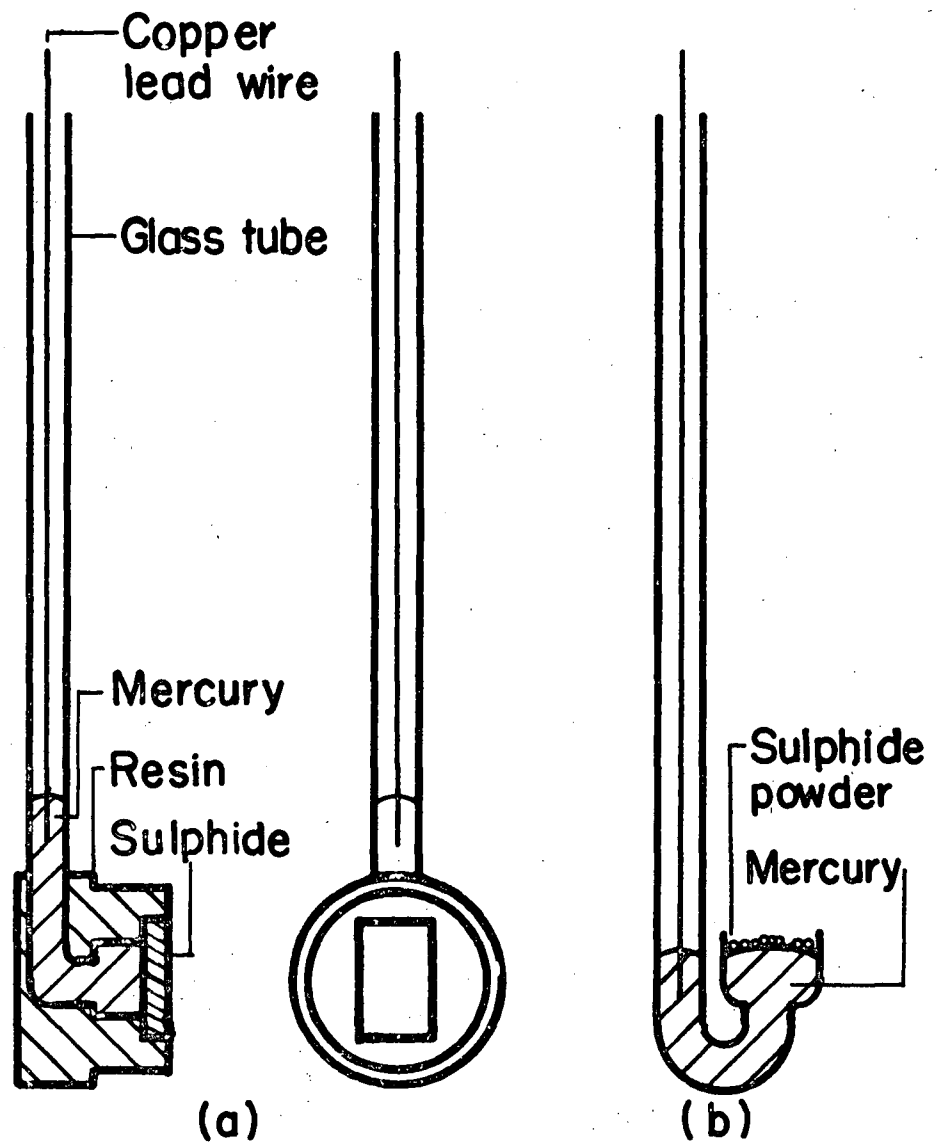
Figure 10. Iron sulphide electrodes

(a) mounted; (b) powder.

According to these data, the powder electrode is suitable for the sulphide electrode, although the values appear more scattered with the powder electrode.

(4) Electrolytic Cell

The rubber bung acting as the top of the cell contained a gas disperser, the sulphide electrode, a Pt-counter electrode, a Luggin capillary with reference electrode, and a gas outlet tube, and was fitted to a 400-ml (tall style) beaker. Usually 250 ml of electrolyte was placed in the beaker and agitated mildly with a magnetic stirrer. In Fig. 11 the sketch for the cell is shown. Potential measurements were made with the KCl saturated calomel electrode as a reference associated with a Luggin capillary. The end of the gas outlet tube was water sealed, so the small positive pressure in the cell caused by the water seal resulted in an improved contact of the sulphide with mercury on which the sulphide powder was floated.

(5) Reagents

The electrolyte solution consisted of 1 M Na_2SO_4 as a buffer, H_2SO_4 for pH control of the solution and $FeSO_4$ of the desired ferrous ion concentration solution.

Helium and hydrogen sulphide gas used were directly passed from both gas cylinders without purification.

(6) Experimental Procedure

Before each run the electrolyte was deoxygenated by bubbling helium

1. Gas out-let tube

2. Pt counter electrode

3. Gas disperser

4. Sulphide electrode

5. Luggin capillary

6. Stirrer magnet
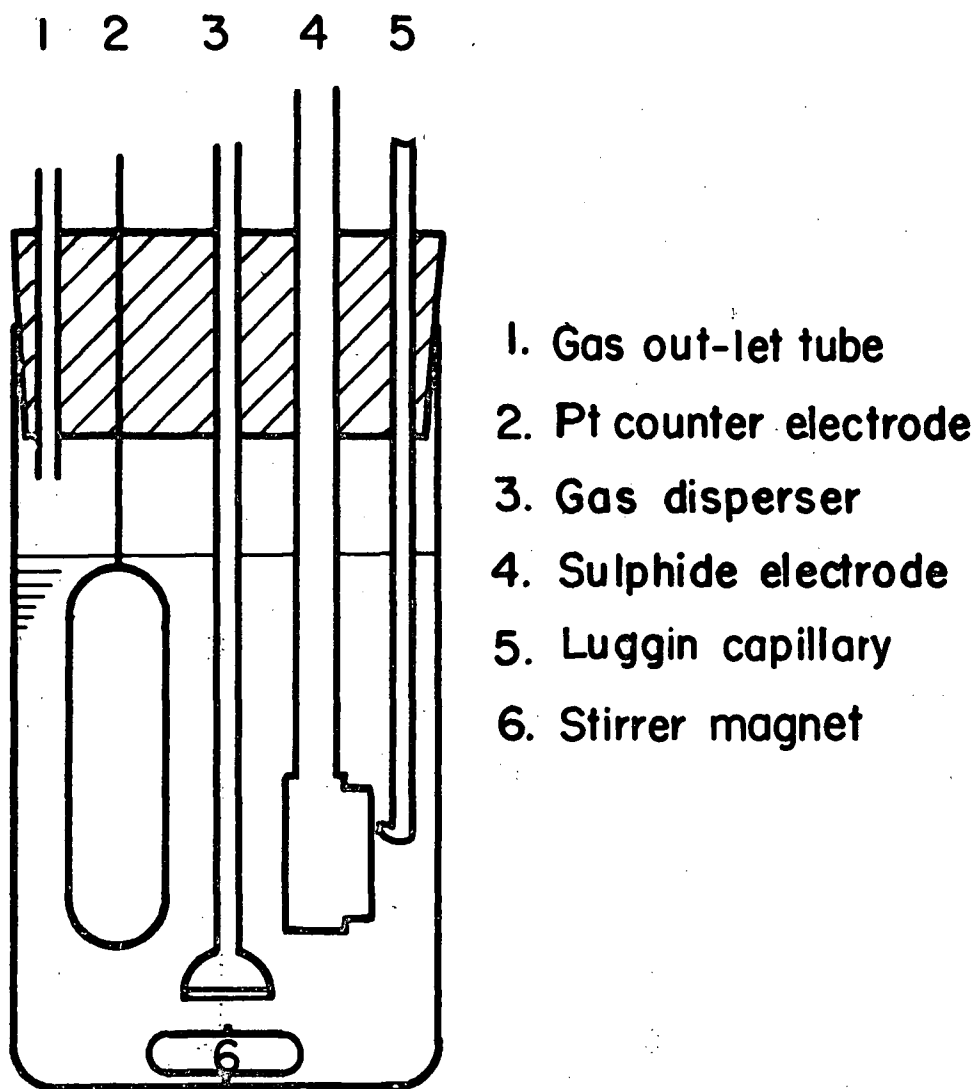
Figure 11. Sketch of electrolytic cell.

gas through it for at least two hours. Then an electrode, either the mounted electrode, which was first polished on emery paper, or the powder electrode, which was first ground in a ceramic mortar under methanol, was immersed into the electrolyte. After a certain period both electrodes were cathodized for 30 minutes at around -400 mV. This cathodic excursion could not be expected to change the composition of pyrrhotite, because the current did not exceed about 1 coulomb.

After the cathodic excursion the rest potential was read at intervals until a stable potential value was obtained, i.e., 1-5 days.

To read potential and to polarize the electrode, a Wenking Standard Potentiostat Model 68 TS10 was used. Fig. 12 shows the relationships of potential with time during the measurement. All potentials were measured against the KCl-saturated calomel electrode, which was taken to be +0.241 volts relative to the standard hydrogen electrode at room temperature, and the potentials are reported on the standard potential scale in this work.

The temperature of the solution was not especially measured and controlled in room temperature experiments. Before and after each run the electrolyte was usually analysed to determine pH and ferrous ion concentration. However, in most cases no significant changes in these values were observed.
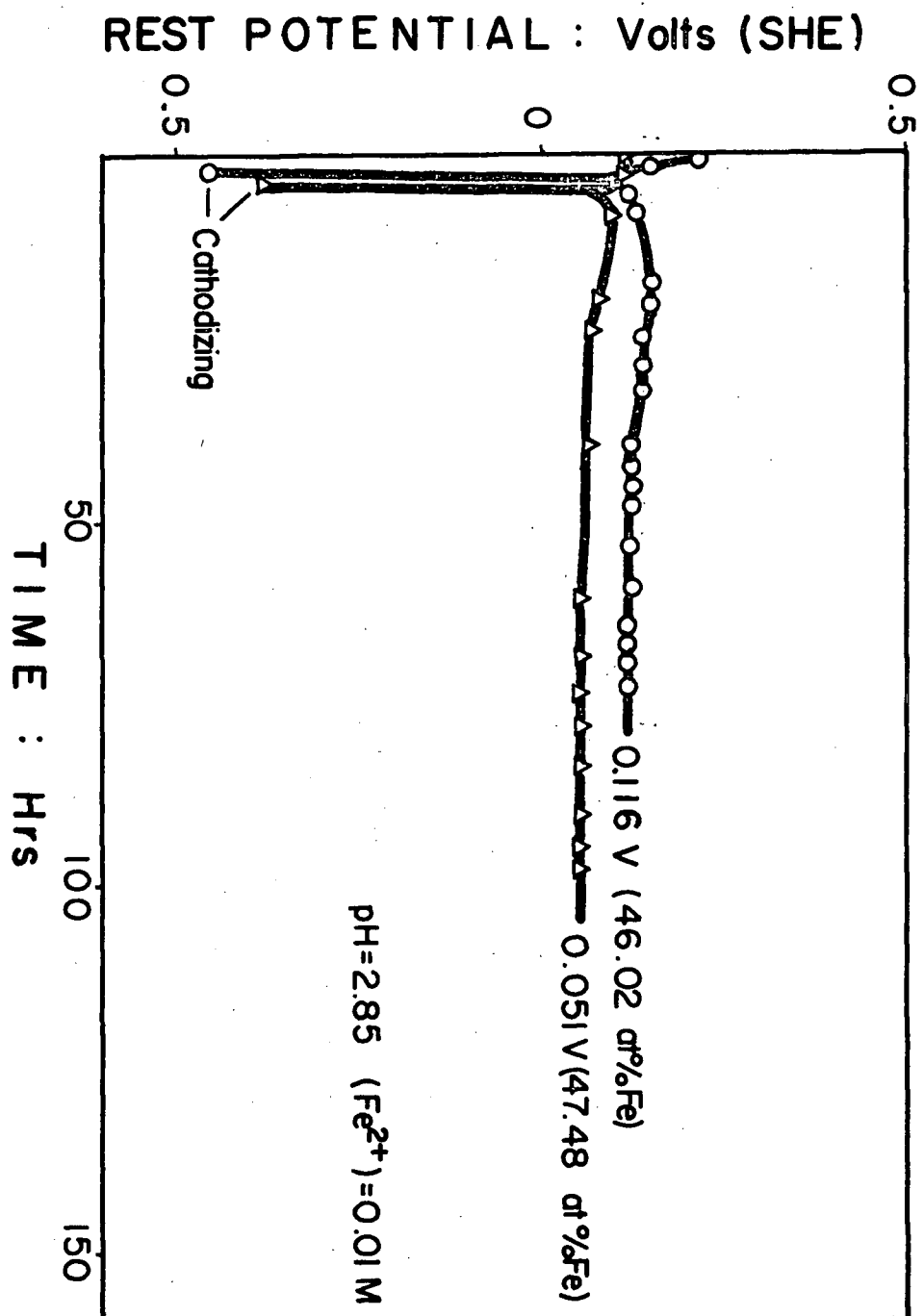
Figure 12. Variation in the rest potential with time.

REST POTENTIAL : Volts (SHE)

TIME : Hrs

Cathodizing

0.116 V (46.02 at%Fe)

0.051V(47.48 at%Fe)

pH=2.85 (Fe²⁺)=0.01M

VI. RESULTS AND DISCUSSION

(1) Effect of Ferrous Ion Concentration

The ferrous ion effect on the rest potential was investigated in the range of concentration of 0.001-0.1 M obtained by addition of $FeSO_4 \cdot 7H_2O$ at approximate pH 2.8 with He bubbling. The ferrous ion concentration was checked before and after each run. However, in most cases no significant change was detected. Fig. 13 shows data obtained for four different stoichiometries of pyrrhotite. The ferrous ion effect on the rest potential is obscure because of scattered data; nevertheless no effect of ferrous ion may be seen for the limiting compositions of 46.2 and 50 atomic percent of pyrrhotites. The experiment in which ferrous ion was increased to 0.01 M from 0.001 M after the measurement of the rest potential in 0.001 M showed no change in the potential, as indicated by arrows in Fig. 13. It may be concluded that ferrous ion does not affect the rest potential significantly. This is supported by K.E. Wrabetz[5] and S. Venkatachalam et al.[7] who found no effect of ferrous ion on the rest potential of the pyrrhotite. At higher concentrations of ferrous ion than 0.1 M at about 2.8 of pH a precipitate formed in the electrolyte, so such concentrations were not used.
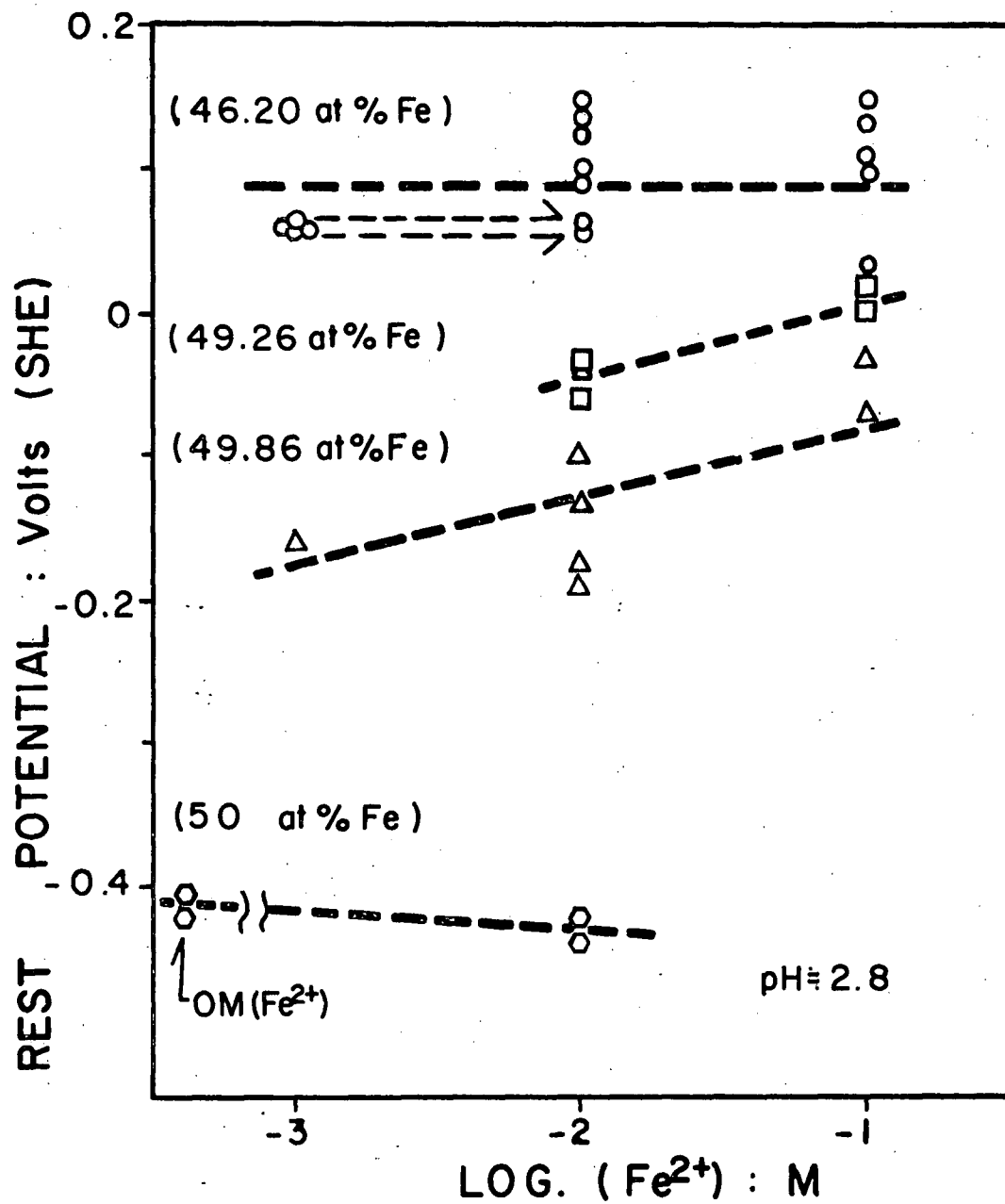
Figure 13. Dependence of the rest potential on ferrous ion concentration.

(2) Effect of pH

In changing pH by addition of sulphuric acid the rest potential of pyrrhotites was measured in the presence of ferrous ion in the electrolyte. The measurements were made on four different stoichiometries of the pyrrhotite. Fig. 14(a)-(c) present the data obtained. It is clear that the rest potential decreases sharply as pH increases. The dependence of pH ranged from about -150 to -350 mV/pH. From these dependences of the rest potential on ferrous ion and pH it is evident that equilibrium between iron in sulphide and ferrous ion in the electrolyte is not established at least in these ranges. If equilibrium were reached, the potential would depend on the ferrous ion concentration and would not depend on pH, according to the Nernst equation (IV-1).

(3) Effect of Hydrogen Sulphide

The next experiment was carried out with hydrogen sulphide bubbled through the electrolyte. Since mercury reacts with hydrogen sulphide to form HgS, the powder electrode could not be used in this experiment, and only the mounted electrode was used. Initially the rest potential was measured in a helium atmosphere, then H_2S was introduced and the rest potential was again measured at a suitable interval. Results are shown in Fig. 15(a) and (b). These data were obtained at pH = 3.01 without ferrous ion in the electrolyte. There are sharp drops in the potential for the natural Chichibu pyrrhotite and the synthesized 47.49 atomic percent Fe pyrrhotite. However, no change in potential was found for the 50 atomic percent synthesized
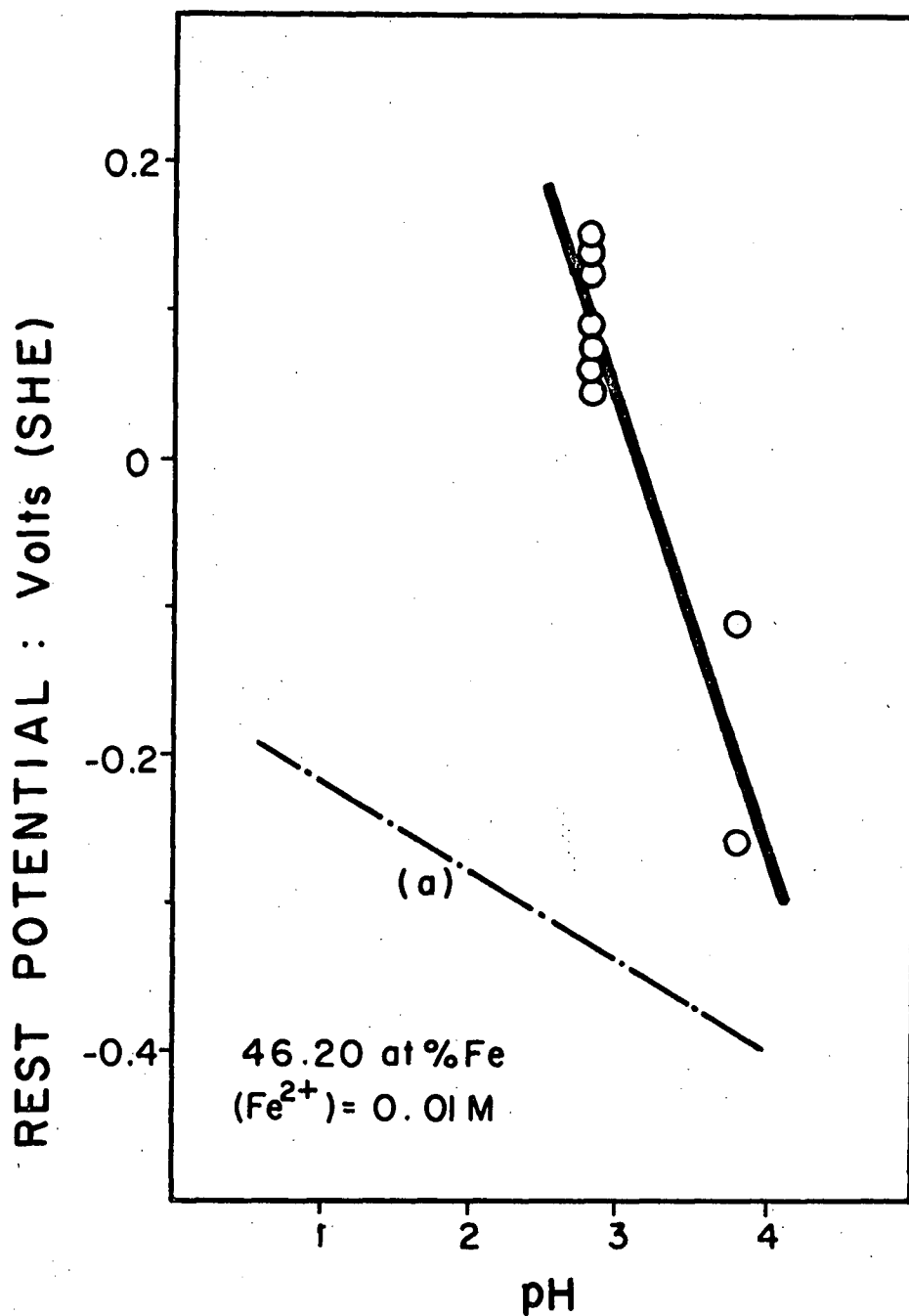
Figure 14a. Dependence of the rest potential on pH

(a); pH-dependence of the reversible potential for

$[S] + 2H^+ + 2e \rightleftarrows H_2S$ calculated from the Nernst equation.
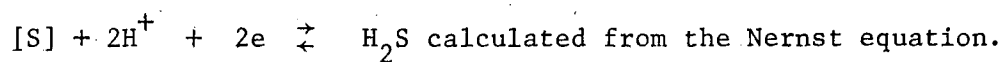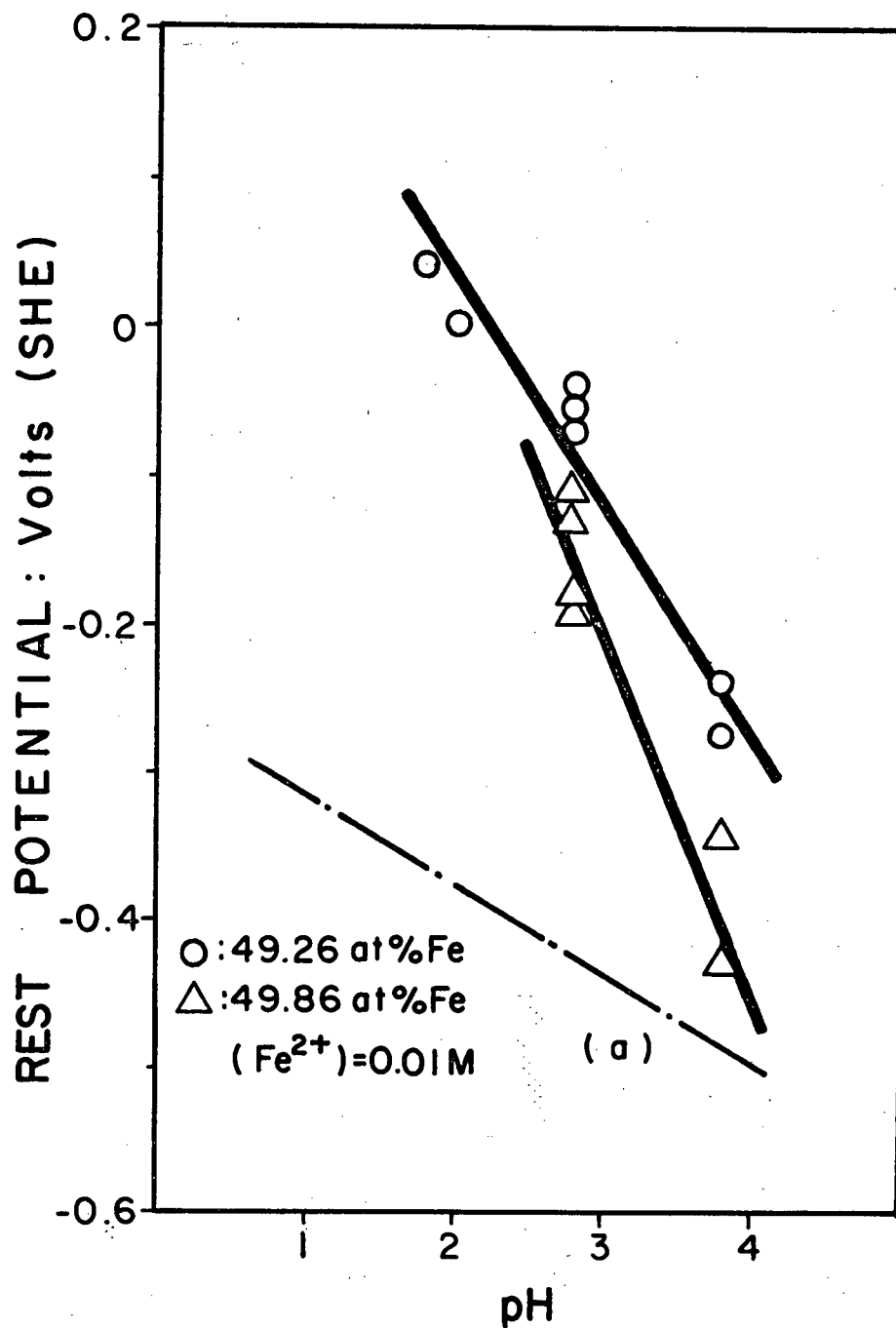
Figure 14b. Dependence of the rest potential on pH.
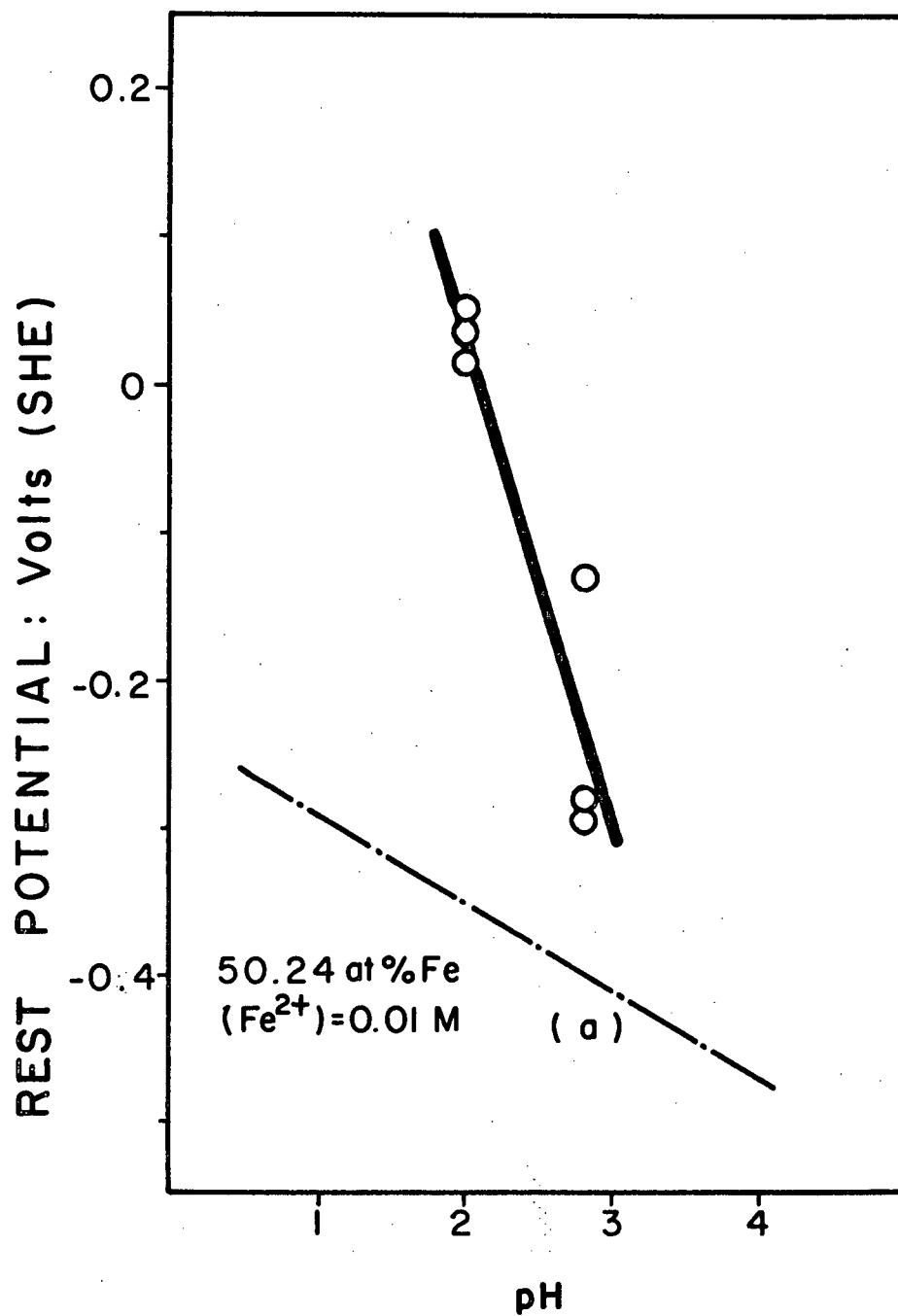
Figure 14c. Dependence of the rest potential on pH.

pyrrhotite even after H_2S introduction. In these experiments before

H_2S bubbling the outlet gas from the cell for the 50 atomic percent

Fe pyrrhotite contained H_2S (as detected by smell), but no H_2S was

detected from the cells containing the other pyrrhotites. All exhaust

gases were passed through a solution containing 1 M Cd ions or Ag

ions, and in all cases yellowish CdS or brown Ag_2S precipitates formed,

although the precipitation rate was much greater for the 50 atomic

percent synthesized pyrrhotite.

According to this experiment, it is possible to make the following

conclusion; for the natural and 47.49 atomic percent Fe synthesized

pyrrhotites the effect of hydrogen sulphide on the potential is large

because of a low hydrogen sulphide evolution rate from the electrodes.

On the other hand, for the 50 atomic percent Fe pyrrhotite the effect

of hydrogen sulphide is not detectable because of a high initial rate

of hydrogen sulphide evolution from the electrode.

(4). Effect of Non-Stoichiometry of Pyrrhotite

The activities of sulphur and iron in the pyrrhotite as well as

the activities of ions in the electrolyte can affect the rest potential,

according to the Nernst equation (IV-1) and (IV-2).*

In this work the rest potential was measured with different

compositions of pyrrhotite at pH $\simeq$ 3 and $[Fe^{++}] = 0.01$ M. The

---

* The effect of activity of the components in a single phase-two
  component electrode has been ignored in most published works on
  sulphide electrochemistry. These activities are very sensitive
  to composition in the single phase region, and as a result cause
  drastic changes in the potential when composition is changed.
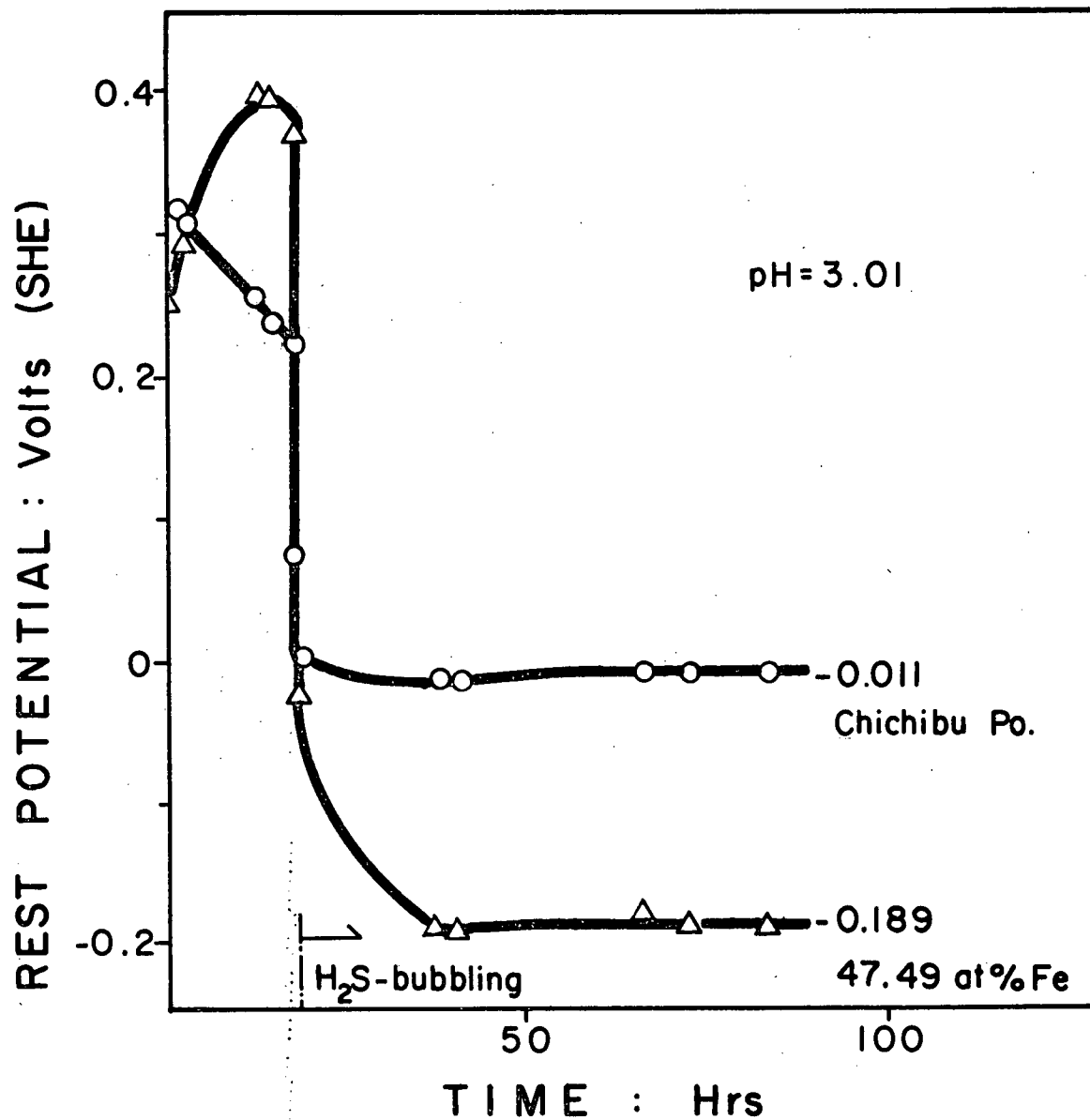
Figure 15a. Rest potential changes in different atmosphere.
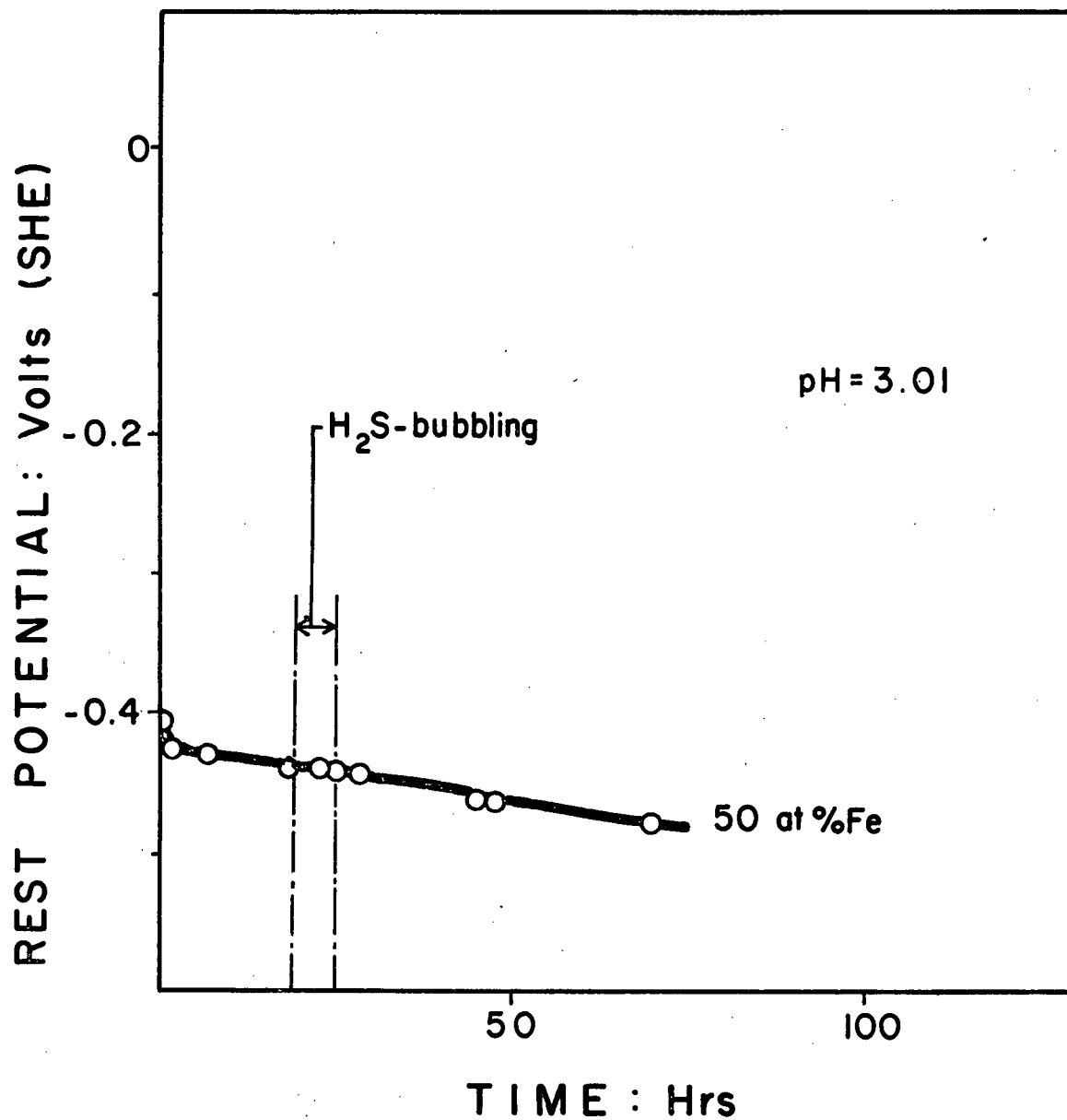
Figure 15b. Rest potential changes in different atmosphere.

results are shown in Fig. 16. From these data, the rest potential varies through a wide range between -350 and +150 mV as the Fe content changes from 50 to 46 atomic percent. In Fig. 16 the potential measured for iron powder on a mercury pool was shown as point (A). Point (B) in Fig. 16 shows the rest potential of the pyrrhotite of 52.8 atomic percent Fe and containing two phases; Fe and FeS. Point (C) in Fig. 16 shows the potential for the mixture of iron powder and the iron saturated pyrrhotite powder. Point (D) shows the rest potential measured for pyrite and Points (E) show the rest potentials of natural pyrrhotite specimens from Chichibu.

Generally natural sulphides have more positive potentials than synthesized sulphides. Pyrrhotite conforms to this generalization. Most sulphides tend towards a non-stoichiometry containing excess sulphur which is more stable under an oxidizing atmosphere. Therefore, natural purrhotite which has been formed at high sulphur activities and later exposed to oxidizing atmospheres will always show a more positive potential than synthesized pyrrhotite formed at high iron activities.

If these rest potentials measured corresponded to reversible potentials, the activity of each component, i.e., sulphur and iron, could be calculated, according to the Nernst equation and the Gibbs-Duhem relationship. However, the possibility of measuring the reversible potential has already been shown to be poor, and so activities were not calculated from the rest potentials.
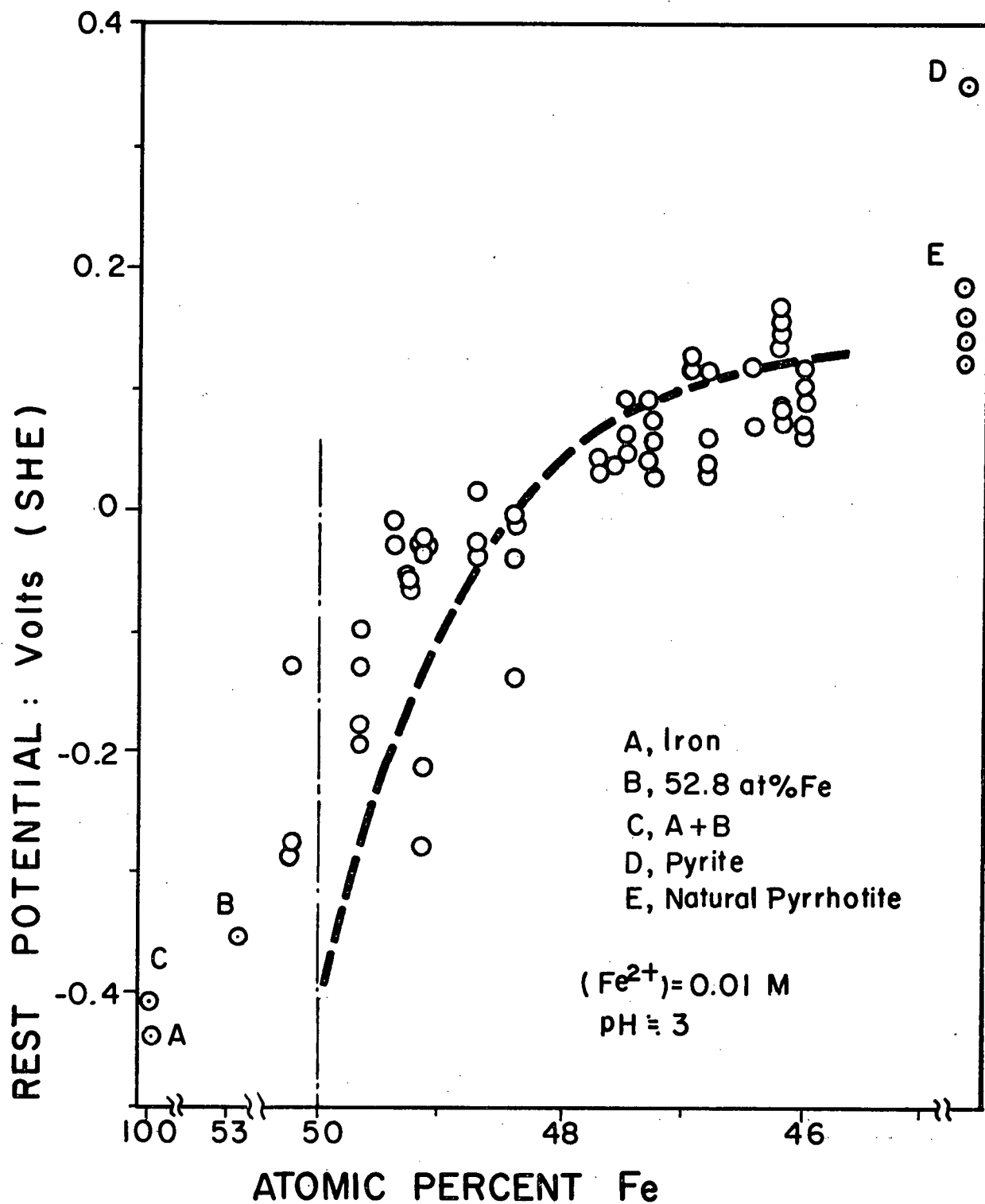
Figure 16. Variation in the rest potential with change in composition of pyrrhotite.

(5) Effect of Residual Impurity in the Electrolyte

In electrochemical experiments it is known that the residual oxidant or reductant in the electrolyte sometimes plays an important role to determine the potential of the electrode even when very dilute. In this experiment, possible oxidants are ferric ion and oxygen gas. The former can come from the ferrous sulphate reagent and the latter can scarcely be avoided from the atmosphere even with He gas bubbling.

The experiment was carried out in the cell shown in Fig. 17 in order to check the effect of residual oxidants in the electrolyte, if they exist, on the rest potential. If oxidants exist in the electrolyte, they can be reduced on the Pt wire cathode during electrolysis. An anode compartment is isolated from the electrolyte with a capillary tube to prevent the migration of oxidant species formed on the anode into the bulk of electrolyte. In Table III data obtained in this cell are compared with those measured in the ordinary cell. The cathodization of electrolyte was continued during the rest potential measurement.

Table III. Comparison of the rest potentials measured with and
without reduction of electrolyte

reduction of electrolyte	measured potentials (mV)
with	+101, +91
without	+139, +147, +91, +80, +150, +60, +50

$[Fe^{++}]$ = 0.01 M, pH = 2.80

cathode potential = −259 mV for

46.2 at % Fe pyrrhotite.

1. Gas out-let &
   Anode compartment
2. Pt cathode
3. Gas bubbler
4. Sulphide electrode
5. Luggin capillary
6. Stirrer magnet
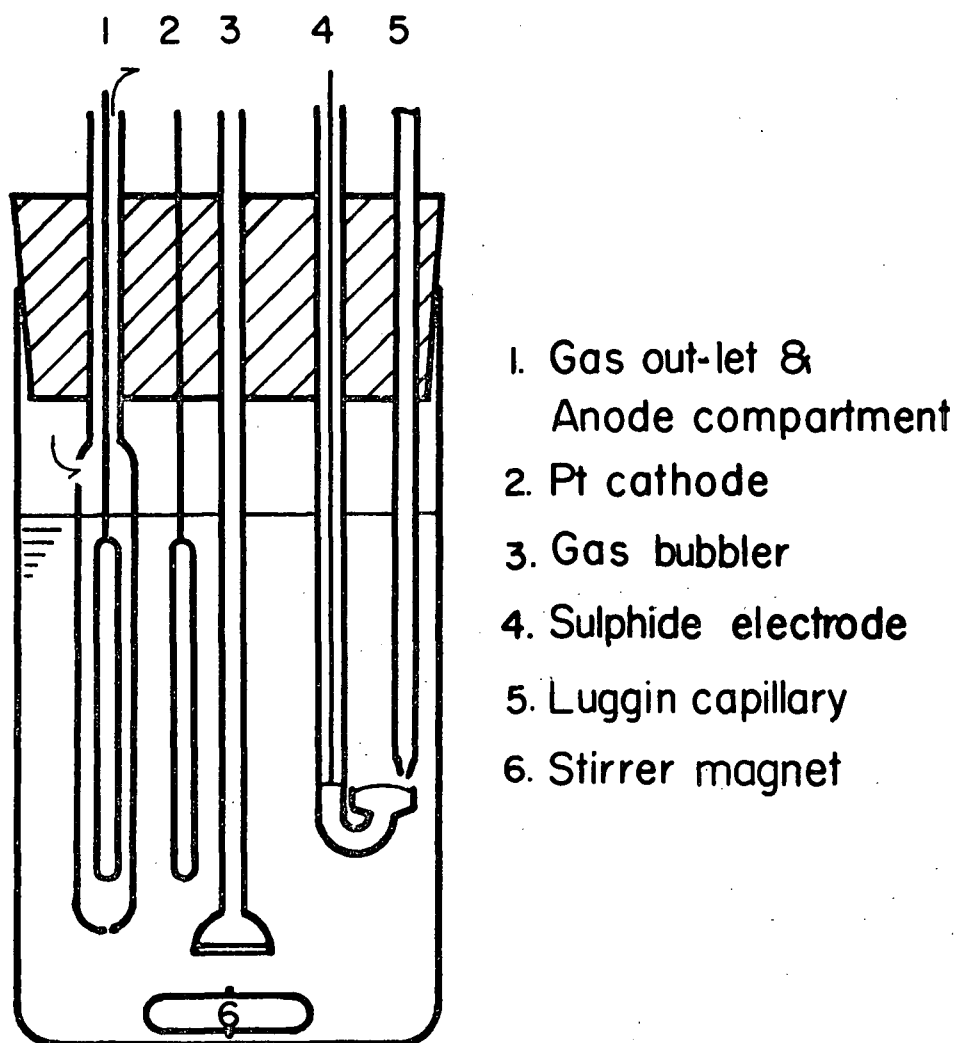
Figure 17. Sketch of the cell for reduction of the electrolyte.

Before and after the run, the pH was checked, but no change in pH was detected. According to Table III, it may be seen that there is no significant change in the potential. Therefore, it may be concluded that either there is no oxidant in the electrolyte or such oxidants as exist do not take part in the potential determing reaction.

(6) Interpretation of the Measured Rest Potential

The behaviour of the rest potential of pyrrhotite can be described as follows:

1) The potential does not depend on the ferrous ion concentration.

2) In the presence of ferrous ion in the electrolyte the potential decreases as pH increases.

3) The H_2S effect on the rest potential is not consistent for pyrrhotites of all compositions, that is, H_2S affects the potential for the pyrrhotites containing excess sulphur, but has no effect on the stoichiometric pyrrhotite.

4) The effect of non-stoichiometry of pyrrhotites on the potential is substantial, i.e. as the excess sulphur content in pyrrhotites increases the potential shifts towards more noble values.

In this respect, the pyrrhotite electrode is different in character in the first three points mentioned above from sulphide electrodes, i.e. for Cu-S, Pb-S and Ag-S systems a metal ion concentration dependence was always obtained and the observed potential was consistent with an equilibrium between metal ions in the electrolyte and metal in the sulphide phase; also H_2S in the electrolyte was apparently in equilibrium with sulphur in the sulphide.[6] The fourth point above is similar to observations by J. Brodie.[16] His measurements are

Figure 18. Experimental variation in the rest potential of galena for low (Pb^{++}) at pH = 0.
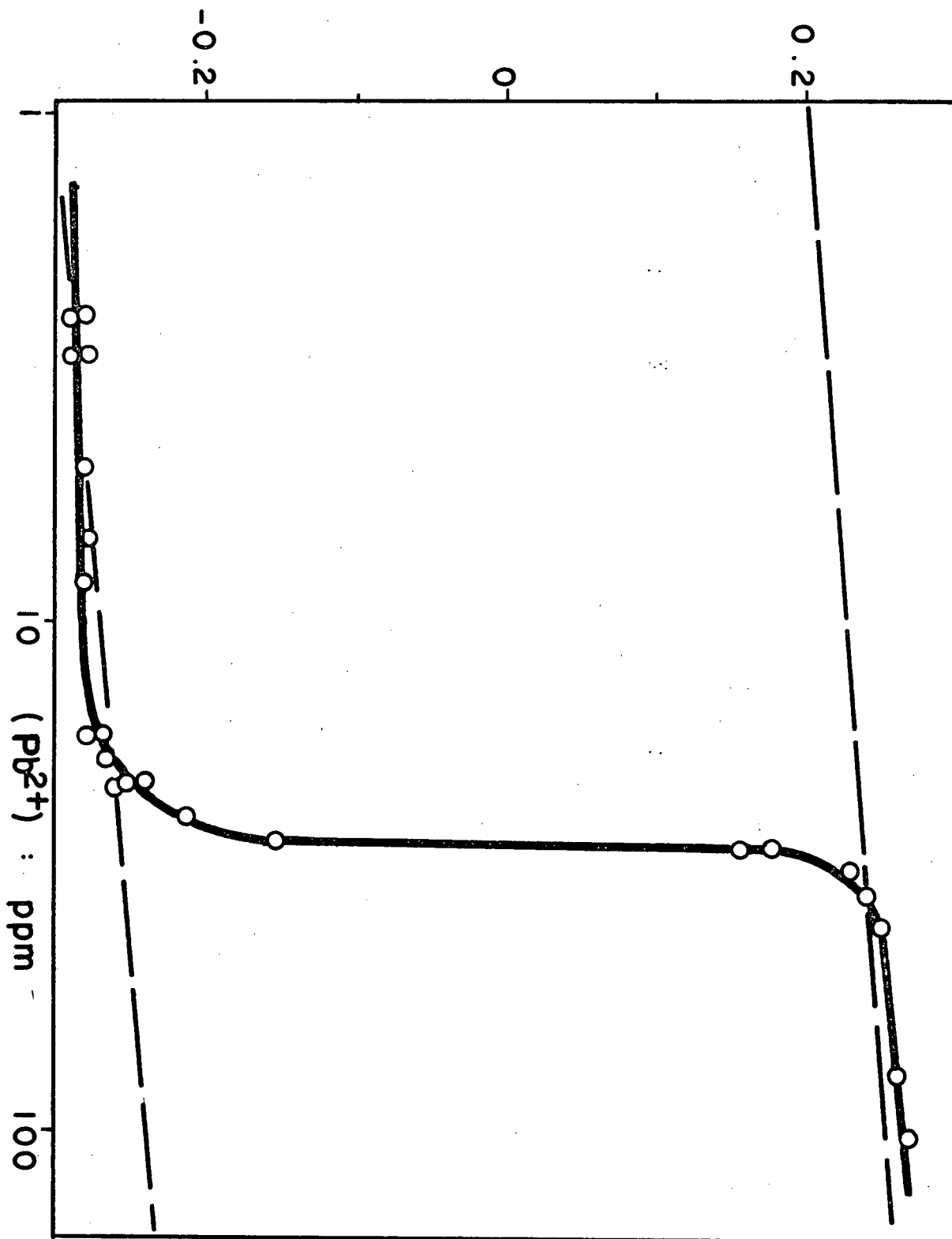
reproduced in Fig. 18. The curve in Fig. 18 was obtained by the
following method; a galena electrode was cathodized with a current
density 1 mA/cm^2 in 1 M HClO$_4$ solution for 1 hr, then anodized in
freshly deoxygenated 1 M HClO$_4$ solution with a current density 1 mA/cm^2.
During anodization the current was interrupted for the measurement
of the rest potential after successive short periods. Meanwhile,
the electrolyte was sampled for Pb^{++} ion analysis. The curve
signifies that galena saturated with Pb metal by cathodization was
gradually changed in composition from metal-rich to sulphur-rich by
anodization, equilibrium between the electrode and the electrolyte
being reached to establish the potential of the galena electrode.
From this curve the effect of composition of galena on the rest
potential is seen, although a quantitative relationship showing the
precise stoichiometry range could not be obtained.

The behaviour of the pyrrhotite electrode will be interpreted
schematically on the current-density potential diagram introduced
earlier. During the following interpretation it is assumed that
concentration polarization will not appear and the kinetic parameters,
i.e. ka, kc, α and β, remain constant as potential changed. In
other words linear relationships of logarithm-current-density vs
potential are maintained. Although these conditions seem to be
oversimplified, it is easier to understand the sulphide electrode
when these assumptions are made.

(6-1) Initially, let us consider the effects of ferrous ion and
hydrogen ion. In Fig. 19(a) the current-density potential relationships
for [Fe] $\rightarrow$ Fe^{++} + 2e,[*] [S] + 2H$^+$ + 2e $\rightarrow$ H$_2$S,[*] and Fe^{++} + 2e $\rightarrow$ Fe are

_____

[*] From here on, iron and sulphur in sulphide phase are expressed as
[Fe] and [S], respectively.

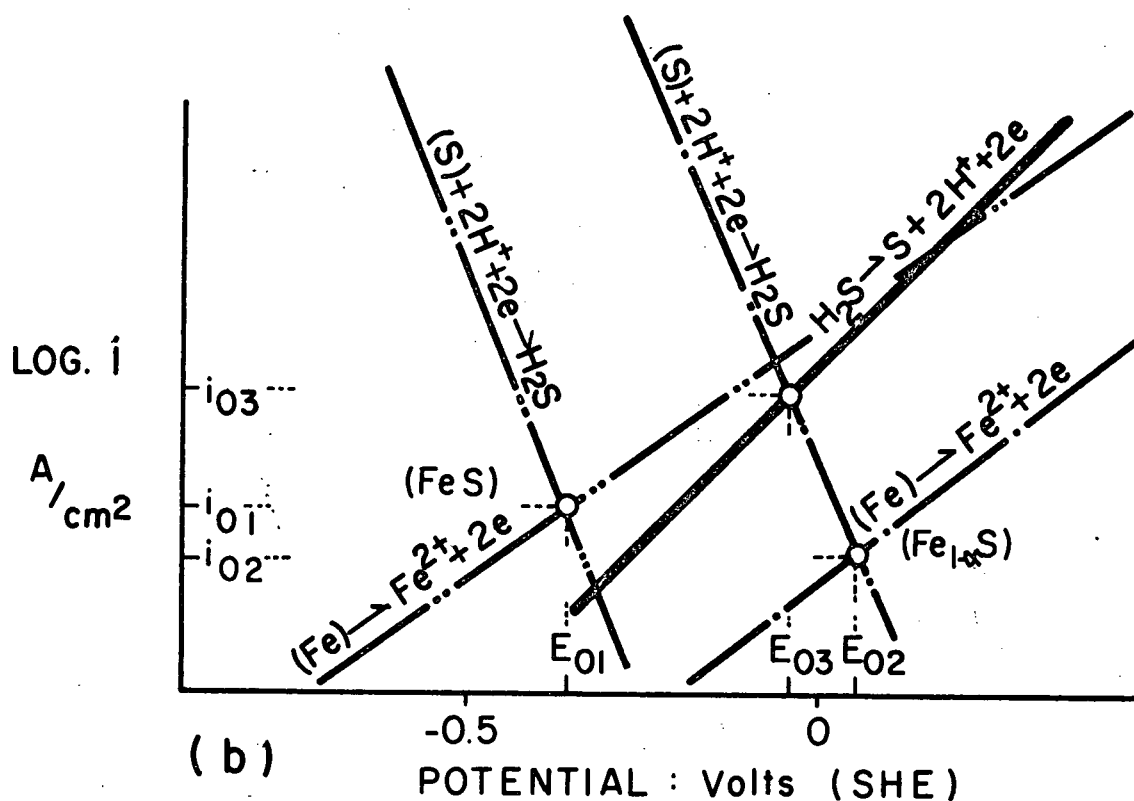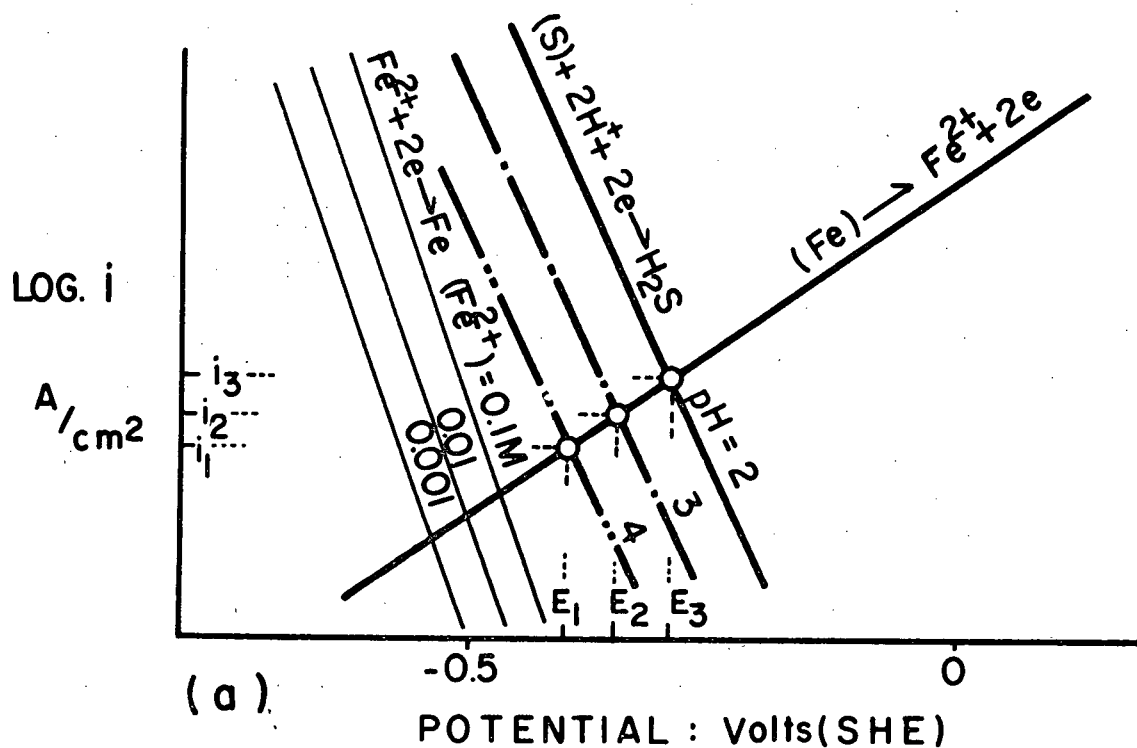Figure 19. Current-density potential relationships for the cell

    (a)   pyrrhotite $|$X-FeSO$_4$, y-H$_2$SO$_4|$S.H.E. (25°C)

    (b)   pyrrhotites $|$H$_2$SO$_4$, He or H$_2$S$|$S.H.E. (25°C).

schematically described. In Fig. 19(a), the line of the cathodic reaction of ferrous ion which is added 0.1 M as a maximum to the electrolyte in order to obtain the reversible potential of $Fe^{++} + 2e \rightleftarrows$ [Fe] is located below the line for the cathodic reaction of $[S] + 2H^+ + 2e \rightarrow H_2S$. Therefore, the potential determining coupled reactions consist of the anodic reaction of $[Fe] \rightarrow Fe^{++} + 2e$ and the cathodic reaction of $[S] + 2H^+ + 2e \rightarrow H_2S$ in the region where the experiment was undertaken. In this case the rest potential of pyrrhotite does not depend on the ferrous ion concentration but it depends on pH because the line for the cathodic process is a function of hydrogen ion concentration. When the pH is decreased, i.e. hydrogen ion concentration is increased, the line for the cathodic reaction shifts upwards lifting the intersection with the anodic line as a result. This causes the increase in potential as pH decreases. The detection of hydrogen sulphide evolution from the cell supports the possibility of $[S] + 2H^+ + 2e \rightarrow H_2S$ as a cathodic process of the potential-determining reactions.

A thermodynamic consideration for the reaction of $FeS + 2H^+ \rightleftarrows Fe^{++} + H_2S$ suggests the possibility of $[S] + 2H^+ + 2e \rightarrow H_2S$ as a cathodic process in the potential-determining reactions of pyrrhotite. In Table IV the equilibrium constants of $M_{2/n}S + 2H^+ = H_2S(aq) + 2/nM^{n+}$ which are calculated from the free enthalpy data from the Latimer[3] are presented. Using the value K for pyrrhotite, when pH is 3, $a_{H_2S(aq)}$ can be calculated in the following way;

$$a_{H_2S(aq)} = 3.55 \times 10^{-4} \times \frac{1}{a_{Fe^{++}}} \qquad \text{(VI-1)}$$

$$i_a = 2F \, k_a a_{Fe} \, \exp \left\{ \frac{2\alpha F \epsilon}{RT} \right\} \qquad (VI-2)$$

and for the cathodic process

$$i_c = -2F \, k_c a_s \, a_{H^+}^2 \, \exp \left\{ - \frac{2\beta F \epsilon}{RT} \right\} \qquad (VI-3)$$

At the equipotential on the pyrrhotite electrode and in the assumption of a steady state, from (VI-2) and (VI-3) the equation

$$i_a = -i_c = 2F \, k_a a_{Fe} \, \exp \left\{ \frac{2\alpha FE}{RT} \right\} = 2F \, k_c a_s a_{H^+}^2 \, \exp \left\{ - \frac{2\beta FE}{RT} \right\} \qquad (VI-4)$$

is obtained, where E is the potential of pyrrhotite.

Equation (VI-4) yields for the pH-dependence of the potential,

$$E = - \frac{1}{\alpha+\beta} \, 0.059(pH) - \frac{2.3RT}{2F(\alpha+\beta)} \, \log \frac{k_a a_{Fe}}{k_c a_s} \qquad (VI-5)$$

According to data of the dependence of the rest potential on pH in this work, i.e. (-150) to (-350) mV/pH, the sum of the transfer coefficients for the cathodic and anodic reactions will be predicted to be less than unity.

(6-2) Secondly, the effect of H_2S on the rest potential is discussed in the same manner using the current-density potential diagram shown in Fig. 19(b). In Fig. 19(b), the possible electrochemical processes are; $[Fe] \rightarrow Fe^{++} + 2e$, $[S] + 2H^+ + 2e \rightarrow H_2S$ and $H_2S \rightarrow 2H^+ + S + 2e$.

Before H_2S bubbling, the rest potential for the 50 atomic percent

Fe pyrrhotite and natural or 47.49 atomic percent Fe pyrrhotites are

shown E_{01} and E_{02} ($E_{02} > E_{01}$), which are determined by the coupled

reactions of $[Fe] \rightarrow Fe^{++} + 2e$ as an anodic process and $[S] + 2H^+ + 2e \rightarrow$

H_2S as a cathodic process. Then, by H_2S bubbling through the electrolyte

the line of the anodic reaction of $H_2S \rightarrow 2H^+ + S + 2e$ appears on the

diagram. As a result, when this new anodic line is lower than the

anodic line of $[Fe] \rightarrow Fe^{++} + 2e$, as is the case for the 50 atomic

percent Fe pyrrhotite, the coupled reactions determining the rest

potential are still $[Fe] \rightarrow Fe^{++} + 2e$ and $[S] + 2H^+ + 2e \rightarrow H_2S$. However,

for the natural and 47.49 atomic percent Fe pyrrhotites, the anodic

line of the reaction $H_2S \rightarrow 2H^+ + S + 2e$ is over the $[Fe] \rightarrow Fe^{++} + 2e$

anodic reaction line, so a new potential is established, as determined

by the coupled reactions of $H_2S \rightarrow 2H^+ + S + 2e$ and $[S] + 2H^+ + 2e \rightarrow$

H_2S. This new potential E_{03}, shown in Fig. 19(b), must be more

negative than E_{02}, having a higher current density i_{03} than i_{02}.

If equilibrium between sulphur in sulphide and sulphur deposited from

the anodic reaction of hydrogen sulphide is established, the equilibrium

potential for $[S] + 2H^+ + 2e \rightleftarrows H_2S$ can be obtained.

(6-3) Thirdly, the behaviour of the non-stoichiometry of

pyrrhotites will be interpreted using the current-density potential

diagram. The observations on the effect of the non-stoichiometry are

these; when the excess sulphur in the pyrrhotite increases, the rest

potential increases and the rate of the hydrogen sulphide evolution

decreases. In consideration of these facts, the current-density

potential relationship is shown in Fig. 20, as a function of the non-stoichiometry of pyrrhotite. When the content of excess sulphur in the pyrrhotite increases, the lines for the cathodic reaction of $[S] + 2H^+ + 2e \rightarrow H_2S$ and the anodic reaction of $[Fe] \rightarrow Fe^{++} + 2e$ shift towards more noble values, because the activity of sulphur increases, while the activity of iron decreases with increase in excess sulphur in the pyrrhotite. As a result the rest potential shown as an intersection of the cathodic and anodic lines moves towards more noble potentials and the value of the exchange current density decreases when the excess sulphur content increases.

(7) Galvanic and Polarization Effect on the Hydrogen Sulphide Evolution

The current-density potential relationship for the cathodic reaction of $[S]+2H^+ + 2e \rightarrow H_2S$ predicts that the rate of the hydrogen sulphide evolution must be affected in the following manner; a) anodic polarization of the pyrrhotite electrode should reduce the rate of hydrogen sulphide evolution, b) cathodic polarization should accelerate hydrogen sulphide evolution. In consequence, when pyrrhotite electrically contacts a material which is lower in potential than the pyrrhotite, H_2S evolution from the pyrrhotite should be accelerated.

Two attempts were carried out to test these predictions. To test for a galvanic effect two kinds of pyrrhotite, one of stoichiometric composition and the other containing excess sulphur were immersed in a cell and the electrical lead wires from both specimens were shorted. The polarization effect on the hydrogen sulphide evolution was studied with an electrode of stoichiometric composition. The rate of hydrogen
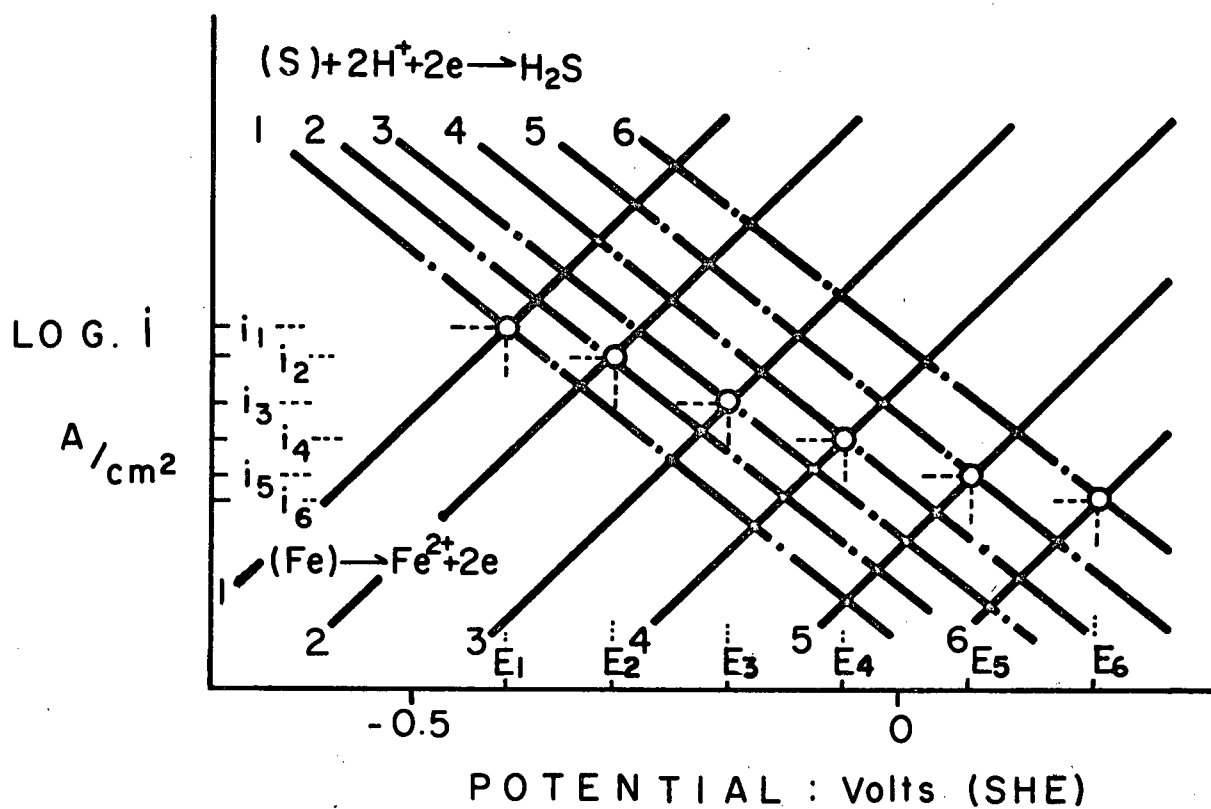
Figure 20. Current-density potential relationships for the cell
different pyrrhotites. $|FeSO_4$, $H_2SO_4|$S.H.E. (25°C).

sulphide evolution was measured in the following way; He carrier gas
from the cell was bubbled through the solution contained 1 M of
$Cd(NO_3)_2$ to collect H_2S gas in the form of CdS precipitate. At 1 or
1/2 hour intervals the CdS precipitate was filtered in a Gooch crucible,
washed, dissolved into 1:1 hydrochloric acid, and analysed for Cd with
an atomic adsorption spectrometer.

In Fig. 21 and 22, the results are shown. A galvanic effect on
the H_2S evolution is obvious, and the anodization of pyrrhotite
decreases the H_2S evolution and the cathodization increases the H_2S
evolution rate. Using an H_2S evolution rate of 2.7×10^{-5} mol/hr
under open circuit conditions in a solution of pH = 2.65 and an
electrode surface area of 2.92 cm^2, the dissolution equivalent current
density was calculated to be 5.0×10^{-4} A/cm^2. This value is much
larger than the value of 10^{-8} A/cm^2 for an iron electrode in 1 M
$FeSO_4$ solution obtained by Roiter et al.[17] This supports the view that
the reversible reaction for $Fe^{++} + 2e \rightleftharpoons [Fe]$ in the stoichiometric
pyrrhotite, where $a_{Fe} = 1$, can not be a potential determining reaction
at this pH.

(8) Electrochemical Mechanism of Leaching Reactions

When the leaching process proceeds in an oxidizing atmosphere,
the cathodic reduction of oxidants becomes part of the sulphide electrode
system. For example, when pyrrhotite is leached with oxygen as a
oxidant, the possible electrochemical reactions include the following;

1) oxidation of iron in pyrrhotite into ferrous ion

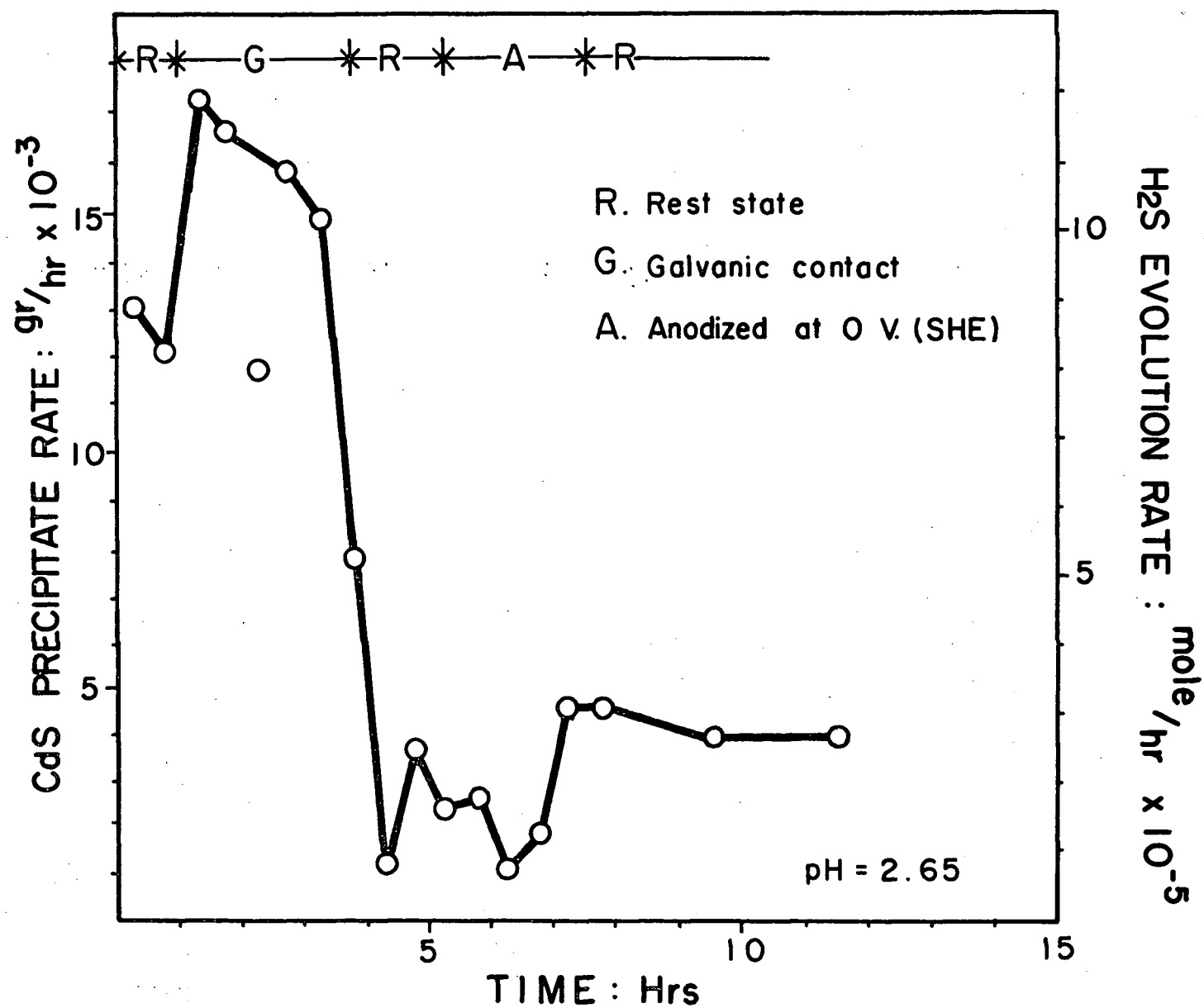$$[Fe] \rightarrow Fe^{++} + 2e$$
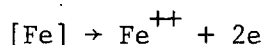
Figure 21. Variation in H_2S evolution rate with a galvanic contact and anodization of pyrrhotite.
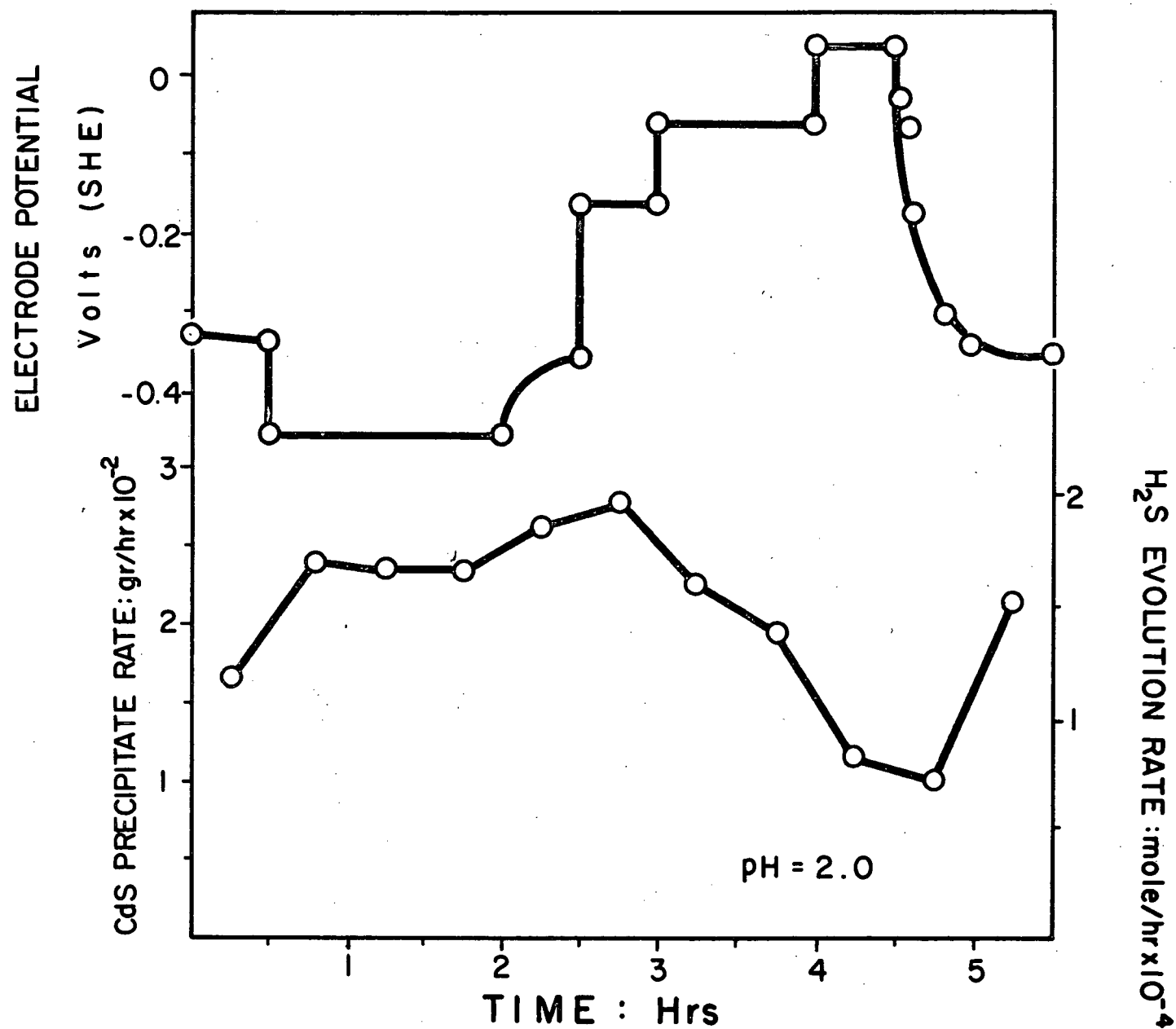
Figure 22. Variation in H_2S evolution rate with change in potential of pyrrhotite electrode.

2) oxidation of sulphur in pyrrhotite into sulphate ion

$$[S] + 4H_2O \rightarrow SO_4^= + 8H^+ + 6e$$
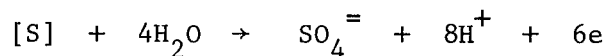
3) reduction of sulphur in pyrrhotite into hydrogen sulphide

$$[S] + 2H^+ + 2e \rightarrow H_2S$$
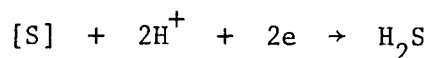
4) reduction of oxygen gas on the sulphide surface,

$$O_2 + 4H^+ + 4e \rightarrow 2H_2O$$
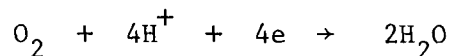
5) oxidation of ferrous ion in solution into ferric ion on the

sulphide surface

$$Fe^{++} \rightarrow Fe^{+++} + e$$
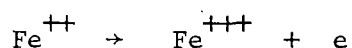
6) reduction of ferric ion in solution into ferrous ion on the

sulphide surface

$$Fe^{+++} + e \rightarrow Fe^{++}$$
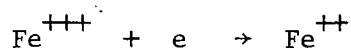
7) oxidation of hydrogen sulphide in solution into elemental

sulphur on the sulphide surface

$$H_2S \rightarrow 2H^+ + S + 2e$$
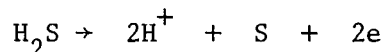
These all possible reactions must be considered, and some of these

reactions, i.e. 4), 5), 6) and 7) can combine as homogeneous electron

transfer reactions occurring remote from the sulphide surface, which

complicates the system still more. However, the reaction potential

on the sulphide surface is determined by coupling of the particular

cathodic and anodic reactions which lead to a maximum exchange current

density in the system. As a result the reaction rates, i.e. the

current densities, for the slower reactions must be controlled by

this potential. In a practical case the concentration polarization effect

must also be considered. If this effect exists, the rates of effected

reactions are determined by diffusional parameters rather than by the electrode potential. Therefore, the analysis of the process of leaching becomes very complicated.

Besides this, an electrochemical study of oxidants must encounter experimental difficulties, because these oxidants often react with the electrode changing its surface condition and, leading to data that are poorly reproducible.

Nevertheless, in the application of electrochemical mechanisms to leaching processes, the form of sulphur as a reaction product can be anticipated;

a) If the potential on the sulphide surface during the leaching is so low that the hydrogen sulphide evolution may occur, the sulphur product is hydrogen sulphide, or when hydrogen sulphide can be oxidized in the solution homogeneously as a sequential process it causes the formation of elemental sulphur or sulphate ion.

b) If the potential on the sulphide is between that of hydrogen sulphide evolution and that of oxidation to sulphate ion, elemental sulphur will remain like an anode slime after the dissolution of metal from the sulphide lattice. This sulphur is particularly resistant to further oxidation, once it has recrystallized from the initial skeleton form representing the sulphur lattice of the mineral.

c) If the potential at the sulphide surface is so high that sulphate can be formed, sulphur in the sulphide may dissolve in the form of sulphate ion, accompanying metal dissolution.*

---

* These potentials, 0.81 V for pyrite[18] and about 1 V for galena[16] were found.

In this case sulphur is obtained as sulphate or a mixture of elemental sulphur and sulphate. This behaviour of sulphur from sulphides in an oxidizing leaching process is illustrated in Fig. 23.
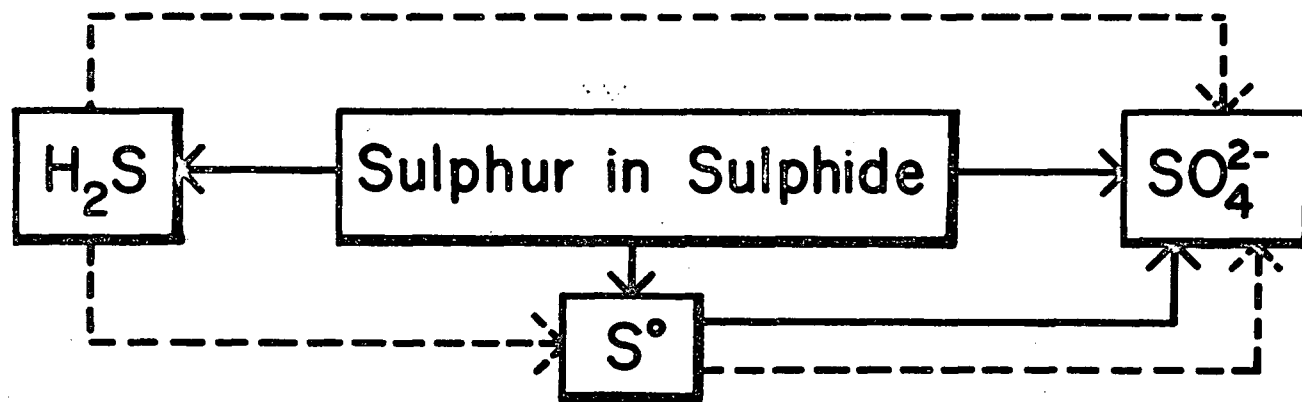
Figure 23. Illustration of the form of sulphur during oxidizing leaching of sulphide minerals.

VII. CONCLUSIONS

(1) The rest potential of pyrrhotite was independent of the ferrous ion concentration in the electrolyte in the range of 0.001 M – 0.1 M.

(2) The rest potential of pyrrhotite was dependent on pH in the range 2 to 4 even in the presence of ferrous ion in the electrolyte.

(3) The H_2S in the electrolyte affected the rest potential of pyrrhotite containing excess sulphur by reducing the potential, but did not have an effect on the rest potential of stoichiometric pyrrhotite.

(4) The effect of non-stoichiometry of pyrrhotite on the rest potential was substantial. Excess sulphur in pyrrhotite increased the rest potential.

(5) A mixed potential of pyrrhotite consisting of the reaction

$$S^o \text{ in pyrrhotite } + 2H^+ + 2e \rightarrow H_2S$$

as a cathodic process and the reaction

$$Fe^o \text{ in pyrrhotite } \rightarrow Fe^{++} + 2e$$
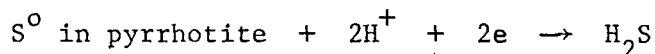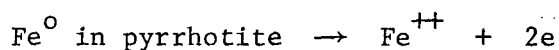
as an anodic process accounts for the character of pyrrhotite electrodes described above.

(6) The hydrogen sulphide evolution from pyrrhotite by acidification may be explained as an electrochemical effect, i.e., a galvanic contact of pyrrhotite with a substance of different potential imposes a polarization on pyrrhotite that either accentuates or suppresses H_2S evolution.

VIII. SUGGESTIONS FOR FUTURE WORK

(1) The rest potentials measured were very scattered. This scatter must be corrected or accounted for so as to interpret the data quantitatively.

(2) The polarization studies of pyrrhotite electrodes are necessary for discussion in more detail. However, it must be considered that the system of sulphide electrodes is more complicated than that of metal electrodes, so the polarization curves obtained may involve those of more than one reaction. In addition, during the polarization of a sulphide such as pyrrhotite which exist in large non-stoichiometric ranges, the composition can change, and this is an essential problem. Composition changes must be avoided for meaningful measurements.

(3) The study of nickel-iron sulphide minerals, i.e. pentlandite, can be undertaken in a meaningful way, only when the pyrrhotite mineral is well understood.

APPENDIX

A. Measurement of the Equilibrium Pressure of H_2S on Pyrrhotite

(1) Introduction

When there is no net current, because of a balance between anodic and cathodic processes, the overall reaction can also be considered as if it were a straightforward chemical reaction with characteristic kinetics and equilibrium.

In the following experiments a measurement of the activity of FeS in pyrrhotite was attempted on the basis of chemical equilibrium with acid solutions. The data on activities of FeS in the non-stoichiometric sulphide are useful for describing thermodynamic functions across the composition range. For the measurement of the activity in sulphides a conventional method is to measure the equilibrium sulphur vapour pressure over the sulphide, either with hydrogen-hydrogen sulphide gas mixtures or with sulphur gas in an inert carrier gas. However, this method can not be applied at low temperatures because of unmeasurably small equilibrium pressures of sulphur over sulphides and probably very slow equilibration rates. Therefore, in this work a measurement of activity was attempted utilizing a reaction of the sulphide with an aqueous solution.

Pyrrhotite may be considered as a binary compound of the components FeS and S. The component of FeS will react with hydrogen ion in the solution according to the following equation:

$$FeS \text{ (in pyrrhotite)} + 2H^+ = Fe^{++} + H_2S(aq) \qquad (1)$$
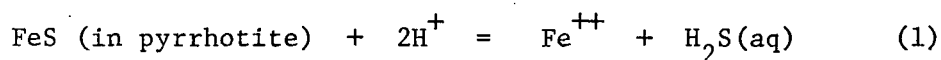
forming ferrous ion and hydrogen sulphide. For this equation, the equilibrium constant can be expressed in the following manner;

$$K = \frac{a_{Fe^{++}} \ a_{H_2S(aq)}}{a_{FeS} \ a_{H^+}^2} \tag{2}$$

The hydrogen sulphide in the solution will equilibrate with hydrogen sulphide in gaseous phase;

$$H_2S(aq) = H_2S (gas) \tag{3}$$

$$K_{(3)} = \frac{P_{H_2S}}{a_{H_2S(aq)}} \tag{4}$$

So, finally Equation (2) yields

$$KK_{(3)} = \frac{[Fe^{++}]P_{H_2S}}{a_{FeS} \ [H^+]^2} = K' \tag{5}$$

where $a_{Fe^{++}}$ and a_{H^+} are assumed to be equivalent to concentrations of each ion.

According to Equation (5), when $[Fe^{++}]$ and $[H^+]$ are known, the activity of FeS can be determined in measuring the pressure of H_2S equilibrated with the system after fixing a standard state. Consequently, the activity of S in the FeS-S binary system can be calculated from the activity data of FeS and the composition of pyrrhotite, using the Gibbs-Duhem integration method for the binary system;

$$\ln a_S = \int_{N_S=1}^{N_S=N_S} - \frac{N_{FeS}}{N_S} \, d\ln a_{FeS} \qquad (6)$$

where N_S and N_{FeS} are mole fraction of S and FeS, respectively.

(2) Experimental

Most thermodynamic studies of sulphides done in aqueous systems at low temperatures have encountered experimental difficulties because of sluggish reaction rates and very small diffusivities in solid state. In this work, a specially designed ball mill was used so as to obtain an equilibrium as soon as possible and avoid a heterogenity in composition of pyrrhotite from the surface to the bulk.

The ball mill was filled to 2/3 of its capacity with solution containing H_2SO_4 and $FeSO_4$, (100 ml volume). 10 gms of powdered pyrrhotite* was sealed into a pyrex glass tube and put in the ball mill to avoid a reaction before the system was deoxygenated. After the whole system was deoxygenated by depressurizing and filled with nitrogen gas at atmospheric pressure, a horizontal shaking action of the ball mill was started.

The pressure of H_2S was measured with an Hg or oil manometer at certain intervals. After a stable H_2S pressure was measured, which usually took 5-10 hrs, the solution was analysed for ferrous ion and pH. The experimental system is illustrated in Fig. 24.
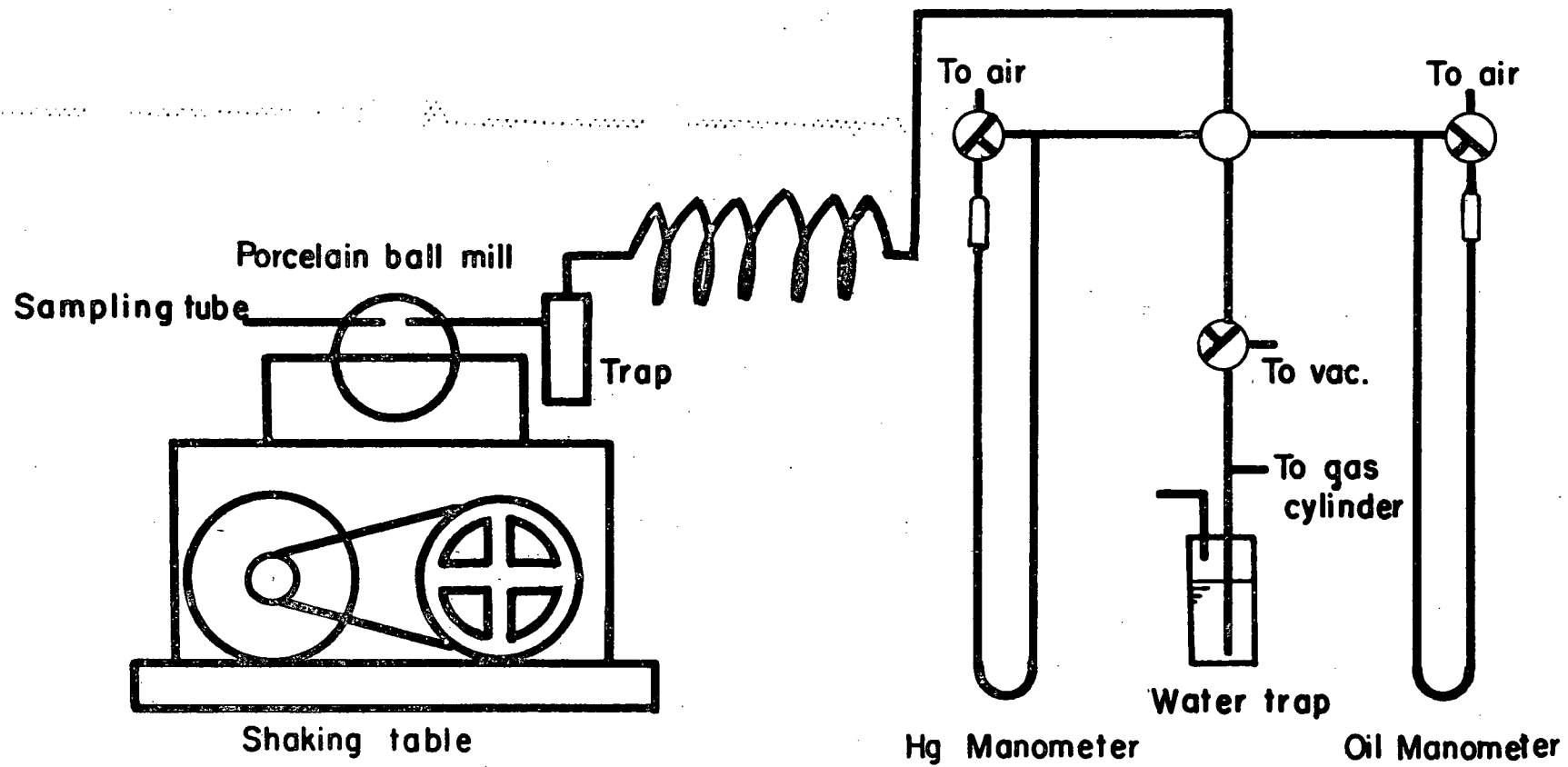
---

* Sullivan pyrrhotite.

Figure 24. Schematic illustration of the equipment for H_2S pressure measurement.

(3) Results and Discussion

In Fig. 25, the variation in H_2S pressure with time is plotted. In this experiment the initial solution contained only 3 cc/l H_2SO_4. According to these curves, the increases in H_2S pressure are fast at the beginning of each run and gradually decreased to a stable pressure. Table V shows the data on H_2S pressure, ferrous ion concentration and pH at equilibrium for initial solutions free of ferrous ion and containing 3 cc/l H_2SO_4, and for 1 M of ferrous ion and 6 cc/l H_2SO_4, respectively. In the same table, from these data the values of $K'' = K'a_{FeS} = [Fe^{++}]P_{H_2S}/[H^+]^2$ are calculated and presented.

The K" values obtained are scattered in the range from 10^3 to 10^6.

Table V. Values of P_{H_2S}, $[Fe^{++}]$, pH and K". Sullivan powder pyrrhotite at 25°C.

Initial solution	P_{H_2S} <cm Hg>	$[Fe^{++}]$ gr/l	pH	K" atm/M
3 cc/l H_2SO_4	10.55	4.18	3.05	1.33×10^4
no $FeSO_4$	8.45	3.30	3.25	2.08×10^4
	7.15	5.64	4.32	4.27×10^6
	6.85	4.70	3.06	1.02×10^4
	6.35	57.00	2.45	6.77×10^3
6 cc/l H_2SO_4	17.40	53.74	2.10	3.50×10^3
	8.62	58.17	2.76	4.55×10^4
1 M $FeSO_4$	27.25	58.22	2.87	2.06×10^5
	24.36	56.84	3.08	4.72×10^5
	18.54	57.22	3.06	1.89×10^5
	27.06	59.22	2.91	2.50×10^5
	22.42	58.06	2.95	2.44×10^5
	27.74	59.28	2.78	1.34×10^5
	15.30	57.67	2.41	1.13×10^4

Figure 25. Increase in H_2S pressure with time.
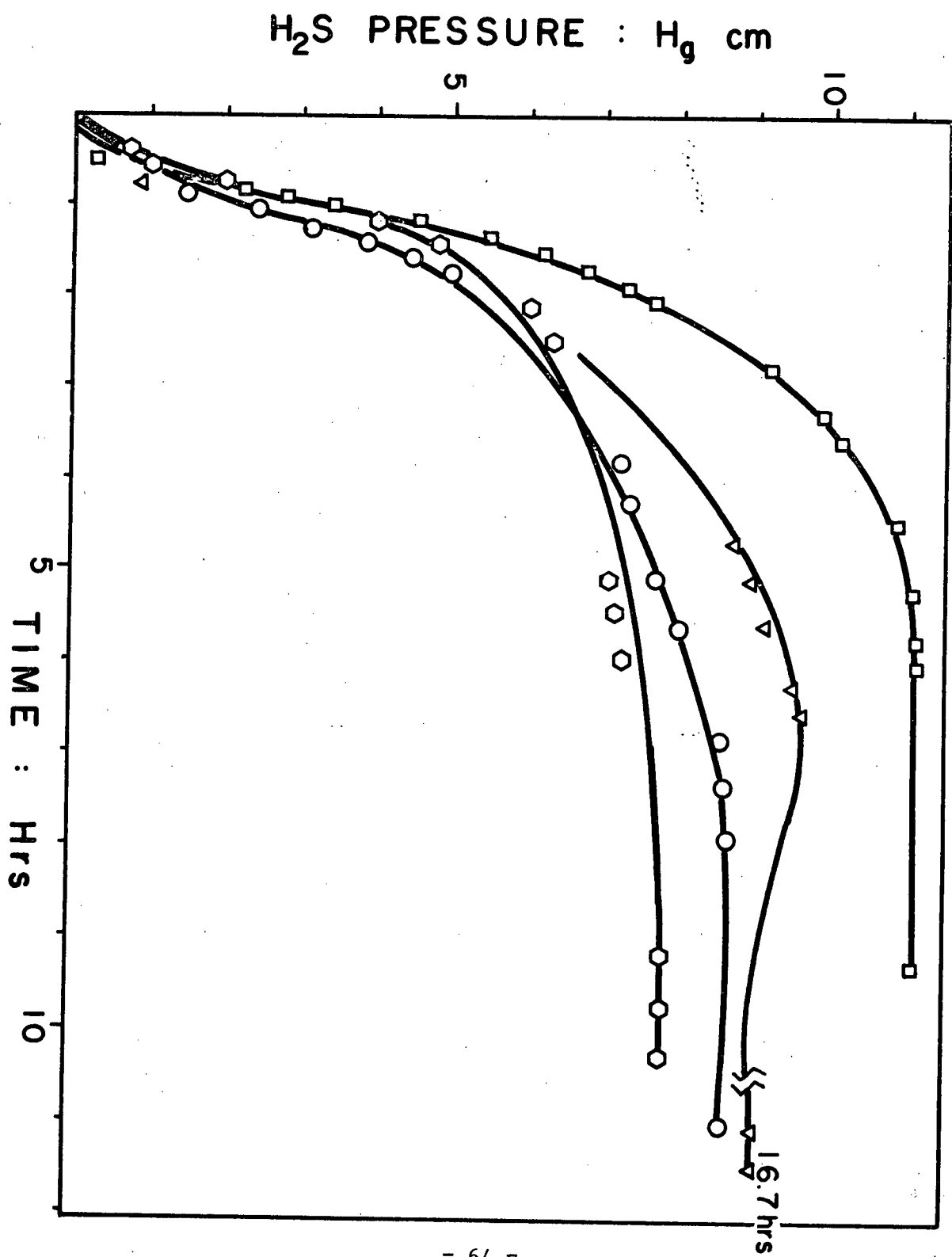
In Fig. 26 these values of K" are plotted as a function of pH. According to Fig. 26, it is seen that the values of K" depend on pH and vary with the initial solution used. The K" values obtained in the initial solution of 1 M $FeSO_4$ and 6 cc/1 H_2SO_4 are larger than those obtained in the initial solution of 3 cc/1 H_2SO_4 and no-$FeSO_4$. The dependence of K" on pH was not expected. Also the wide variation in pH of the final solutions was not reasonable when the same initial solutions were used.

The reason for these unexpected results may be that there is a problem in sampling the final solution. Usually the final solution was drained through the sampling tube after leading nitrogen gas into the ball mill, then the solution was filtered in a Gooch crucible, with an asbestos filter base. During this filtering process of 2-5 minutes the reaction between acid and pyrrhotite suspended in the solution sampled would be possible, because this filteration was conducted under a hydrogen sulphide-free atmosphere with evacuation.

If this reaction occurred, the concentrations of hydrogen ion and ferrous ion in the filtrate solution would differ from those in the solution sampled, and vary with different periods in which the sampled solution was exposed to a free-hydrogen sulphide atmosphere. Furthermore, high dissolution rates of ferrous sulphide[8] and zinc sulphide[19] in acid solutions are reported. The more accurate results to be obtained, the avoidance of possible reaction between pyrrhotite and acid during the sampling process is necessary.
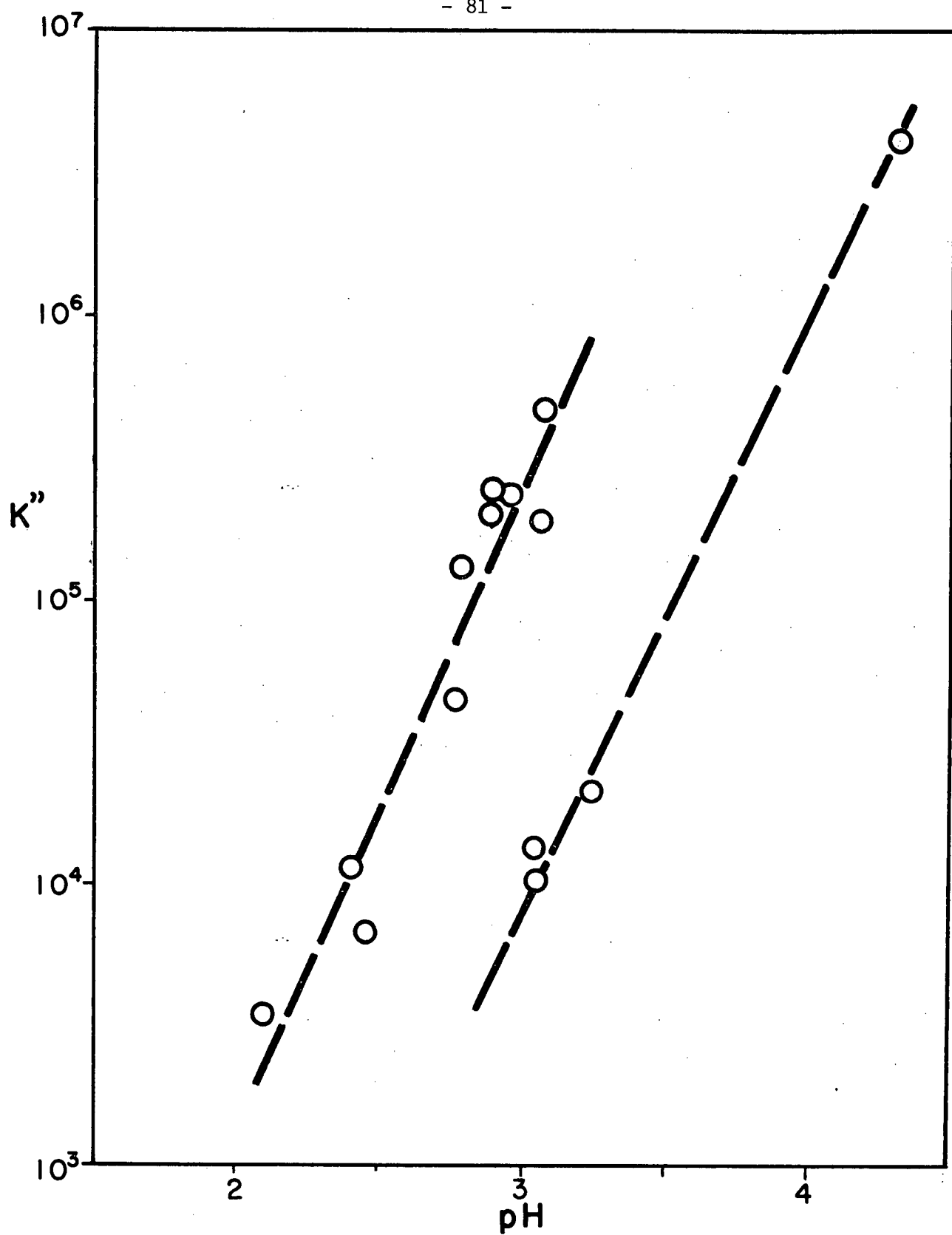
Figure 26. Dependence of K" on pH.

B.

Table VI. Dependence of the rest potential on ferrous ion concentration
at pH = 2.8 at 25°C (for Fig. 13).

Fe content in pyrrhotite ([Fe^{++}] M)	0.001 M	0.01 M	0.1 M
	mV	mV	mV
46.2 at % Fe	+055 , +046	+060 , +150	+151
	+053 , +046	+050 , +147	+135
		+139	+120
		+091	+095
		+080	+035
49.26 at % Fe		−045	+016
		−055	+009
		−059	
49.86 at % Fe	−159	−099	−029
		−129	−069
		−179	
		−189	
50. at % Fe	no [Fe^{++}]		
	−411	−425	
	−420	−440	

C.

Table VII. Dependence of the rest potential on pH, at 25°C,

$[Fe^{++}] = 0.01$ M (for Fig. 14)

Fe content in pyrrhotite at % Fe	pH	the potential (mV)	Fe content in pyrrhotite at % Fe	pH	the potential (mV)
46.2	2.8	+150	49.86	2.8	-099
		+147			-129
		+139			-179
		+091			-189
		+080			
		+060		3.8	-339
		+050			-429
	3.8	-109	50.24	2.0	+051
		-259			+041
					+021
49.26	1.8	+041			
				2.8	-130
	2.0	000			-279
					-285
	2.8	-045			
		-055			
		-059			
	3.8	-239			
		-274			

D.

Table VIII. Variation in the rest potential with change in composition
of pyrrhotite at 25°C, pH ≠ 3 and [Fe^{++}] = 0.01 M
(for Fig. 16)

Fe content at % Fe	the potential mV	Fe content at % Fe	the potential mV	Fe content at % Fe	the potential mV
46.02	+116	47.26	+ 75	48.72	+015
	+111		+ 70		−027
	+091		+ 60		−035
	+071		+ 43		
	+061		+ 41	49.16	−025
					−030
					−035
46.20	+150	47.30	+ 91		−038
	+147		+ 41		
	+139				−215
	+091	47.48	+ 91		−279
	+080		+ 61		
	+060		+ 51	49.26	−045
	+050				−055
		47.57	+ 41		−059
46.43	+116				
	+071	47.72	+ 36	49.39	−010
			+ 33		−030
46.80	+116				
	+060	48.41	−005	49.67	−099
	+038		−010		−129
	+033		−040		−179
46.95	+126		−139		−189
	+121				
50.24	−139				
	−279				
	−285				
(A) iron powder	−434				
(B) 52.8 at % Fe	−354				
(C) (A)+(B)	−419				
(D) pyrite	+347				
(E) Chichibu pyrrhotite (natural)	+186				
	+161				
	+143				
	+124				

REFERENCES

1. Kullerud, G. Research in Geochemistry, Volume II.

2. Yund, R. and Hall, H. Mat. Res. Bull. 3, 779 (1968).

3. Latimer, W.M. Oxidation potentials, Prentice Hall Inc.

4. Majima, H. unpublished work.

5. Wrabetz, K.E. Zeit. fur Elektrochem. 60, 722 (1956).

6. Sato, M. Economic Geology, 55, 1202 (1960).

7. Venkatachalam, S. and Mallikarjunan, R. Trans. of Inst. of Min. and Met. 79, C181 (1970).

8. Pohl, H.A. J. Amer. Chem. Soc. 76, 2182 (1954).

9. Downes, K.W. and Bruce, R.W. Trans. CIMM 58, 77 (1955).

10. Gerlach, J., Hahne, H. and Pawlek, F. Erzmetall. 18, 73 (1965).

11. Vetter, K. Electrochemical Kinetics, Academic Press.

12. Conway, B.E. Theory and Principles of Electrode Processes, The Ronald Press Co.

13. West, W.A. and Menzies, A.W.C. J. of Phys. Chem. 33, 1880 (1929).

14. Haraldsen, H. Zeit. anorg. und allgem. Chem. 246, 169 (1941).

15. Conway, B.E. Electrochemical Data, Elsevier Publishing Co.

16. Brodie, J. Thesis of M.A.Sc. U.B.C. (1969).

17. Roiter, Acta Physicochim, 10, 389 (1939).

18. Peters, E. and Majima, H. Canadian Met. Quarterly 7, 111 (1968).

19. Romankiw, L.T., De Bruyn, P.L. Unit Process in Hydrometallurgy, Group A, p. 45.